

University of Louisville

## ThinkIR: The University of Louisville's Institutional Repository

---

Electronic Theses and Dissertations

---

8-2019

### Triple-junction Solar Cells : in parallel.

Levi C Mays

*University of Louisville*

Follow this and additional works at: <https://ir.library.louisville.edu/etd>



Part of the [Electromagnetics and Photonics Commons](#), [Power and Energy Commons](#), and the [Semiconductor and Optical Materials Commons](#)

---

#### Recommended Citation

Mays, Levi C, "Triple-junction Solar Cells : in parallel." (2019). *Electronic Theses and Dissertations*. Paper 3247.

<https://doi.org/10.18297/etd/3247>

This Master's Thesis is brought to you for free and open access by ThinkIR: The University of Louisville's Institutional Repository. It has been accepted for inclusion in Electronic Theses and Dissertations by an authorized administrator of ThinkIR: The University of Louisville's Institutional Repository. This title appears here courtesy of the author, who has retained all other copyrights. For more information, please contact [thinkir@louisville.edu](mailto:thinkir@louisville.edu).

# Triple-Junction Solar Cells: in Parallel

By Levi Mays

University of Louisville J.B. Speed School

ECE Department

Research Mentor: Shamus McNamara

University of Louisville J.B. Speed School

[shamus.mcnamara@louisville.edu](mailto:shamus.mcnamara@louisville.edu)

## Abstract

This paper looks into the current inefficiency of solar cells and attempts a few alternative solar cell structures in order to provide a more effective source of renewable energy. Currently, multi-junction solar cells are being developed to capture the sun's light more efficiently. One of the ideas in this paper is to add a window to see if the addition of such a layer into a junction will increase the voltage while maintaining nearly the same current output. Central to this paper is the rearranging of the conducting layers of the multi-junction cell so that the junctions can be connected in parallel rather than in series, summing current rather than voltage. We tested if this alternative arrangement produces enough current to over-compensate for the loss in voltage. Also, a hybrid cell structure which mixes parallel and series inter-junction connections was briefly investigated. Out of these different ideas, the windowless parallel design holds the most promise with the hybrid design coming in second place. Given some optimization and fabrication, there may be more efficient solar cells on the market featuring multi-junctions with parallel inter-connections.

# Contents

Abstract.....	1
List of Figures.....	3
List of Tables .....	5
Preface .....	6
Chapter 1 : Introduction .....	7
1.1 Light Absorption in Semiconductors .....	7
Chapter 2 : Design .....	16
2.1 Material Selection .....	17
2.2 Doping Concentration and Layer Thickness Calculations.....	22
Parallel Triple-Junction, Using Heterojunctions.....	24
Parallel Triple-Homojunction .....	27
Series Triple-Homojunction.....	29
2.3 Desired Contact Workfunction Calculations .....	30
Parallel Triple-Junction, Using Heterojunctions.....	31
Parallel Triple-Homojunction .....	31
Series Triple-Homojunction.....	32
Results.....	35
Homojunction vs Heterojunction.....	35
Parallel vs Series (vs Hybrid).....	40
Conclusions.....	48
Works Cited .....	49
Appendix.....	50

## List of Figures

Figure 1	Used and Unused Solar Spectrum for Silicon	p8
Figure 2	Photoelectric Interactions	p8
Figure 3	Solar Cells of Increasing Junctions	p9
Figure 4	Equivalent Circuits for Series & Parallel Arrangements	p10
Figure 5	Equivalent Circuit for Current Sources	p10
Figure 6	Equivalent Circuit for Voltage Sources	p11
Figure 7	Fermi-level Splitting	p12
Figure 8	Solar Cells with Increasing Built-In Voltage	p13
Figure 9	Degenerate Doping	p13
Figure 10	I-V & P-V Curve for an Unspecified Solar Cell	p14
Figure 11	Electric Field & Effective Field	p15
Figure 12	Solar Spectrum Distributions	p16
Figure 13	Short-Circuit Current Density vs Bandgap Value	p17
Figure 14	Parallel Geometries	p18
Figure 15	Absorbed Photons vs Layer Depth	p19
Figure 16	Simplified Solar Cell with Ideal Parallel Geometry	p19
Figure 17	Basic Anti-Reflective Layer Illustration	p21
Figure 18	Diffusion Length in Silicon vs Doping Density	p28
Figure 19	Band Diagram Segment of a Series Triple-Junction Cell	p30
Figure 20	Elaborate Cell Design	p33
Figure 21	Elaborate Cell Band Diagram	p34
Figure 22	Cross-Section of Single Silicon Homojunction Cell	p36
Figure 23	IV Characteristics of Single Silicon Homojunction Cell	p36
Figure 24	PV Characteristics of Single Silicon Homojunction Cell	p37
Figure 25	Extracted Values of Single Silicon Homojunction Cell	p37
Figure 26	Cross-Section of Single Silicon Heterojunction Cell	p38
Figure 27	IV Characteristics of Single Silicon Heterojunction Cell	p38
Figure 28	PV Characteristics of Single Silicon Heterojunction Cell	p39

Figure 29	Extracted Values of Single Silicon Heterojunction Cell	p39
Figure 30	Cross-Section of Parallel Cell	p40
Figure 31	IV Characteristics of Parallel Cell	p41
Figure 32	PV Characteristics of Parallel Cell	p41
Figure 33	Extracted Values of Parallel Cell	p42
Figure 34	Cross-Section of Series Cell	p42
Figure 35	IV Characteristics of Series Cell	p43
Figure 36	PV Characteristics of Series Cell	p43
Figure 37	Extracted Values of Series Cell	p44
Figure 38	Simplified Solar Cell with a Hybrid Geometry	p45
Figure 39	Cross-Section of Hybrid Cell	p45
Figure 40	IV Characteristics of Hybrid Cell	p46
Figure 41	PV Characteristics of Hybrid Cell	p46
Figure 42	Extracted Values of Hybrid Cell	p47

## List of Tables

Table 1	P-N Junction Material Properties	p20-21
Table 2	Anti-Reflective & Contact Material Properties	p22
Table 3	Calculated Design Values	p32

## Preface

What is the greatest pleasure of being an engineer? It's not competition, job security, or travel opportunity. It's certainly not designing for failure nor is it providing rote entertainment. It is nothing hedonistic. No, I believe the divine pleasure of being an engineer is to apply the sciences in order to help others and enable others to be helpful themselves. I believe it is to exorcise the suffering on earth. Second to that and often entailed is the act of creation. However, there are no free lunches in this universe and such pursuits require, fundamentally, energy.

The energy industry is a funny business. It is perhaps the biggest market and is consistently increasing in demand, yet is doomed to collapse given that there are only so many things we can burn in this universe. Ironically, opposite to the energy industry is the war industry which intends to find peace and end itself, and yet our complexes continue its market. Whether we end by war or by famine, I suppose one noble accomplishment would be to design the world so that it burns more slowly. In the case of solar energy, that means taking advantage of something that is already aflame. All on its own, orbiting us, is a star that burns brightly: the Sun. The difficulty is that it is far out of reach. Babel couldn't reach it, and Icarus couldn't touch it. Most of its energy radiates away from Earth into empty space. However, the amount of energy from the Sun that manages to reach the Earth's surface is immense, and the market for photovoltaics is getting riper. This is especially the case for civilizations near the equator such as in Egypt and India.



## Chapter 1 : Introduction

Improved gain from solar energy promises a better future, but a big problem with current photovoltaics is the cost. It doesn't produce enough energy to pay for itself within a reasonable time frame. The average 6-kilowatt residential system costs \$18,300 and won't pay for itself until after 15 years, and that's with the optimistic assumption that the system will fully cover the yearly average bill of \$1200-\$1300 for electricity (Matasci). To make bad news worse, 15 years is half of the product's life. This means an investment in solar energy for a home took 30 years to save \$18,300, which is under \$700 per year. This won't attract many, especially not those who live in cloudier climates where the 'optimistic assumption' mentioned earlier does not apply. Commercially available silicon solar cells have an efficiency that ranges from 14-21% (Aggarwal). What explains this lack of efficiency? Where does the rest of this energy go? There are many answers to this, but this paper will focus on the release of heat by a solar cell when absorbing photons whose energy exceeds the solar cell's threshold.

In this paper, the aforementioned inefficiency will be analyzed from the perspective of the electron energy bands. Additionally, some recent work to improve the situation will be surveyed. This recent work involves adding multiple light-absorbing layers of different semiconductors. I propose a solar cell design of three such light-absorbing layers, and whereas these layers are usually arranged in series I'd like to instead suggest a parallel arrangement in addition to deciding which materials are most fit for such a design. Further, I'd like to prevent the multiple absorber layers from working against each other. This thesis will start with broader conceptual ideas, followed by more specific design choices, calculations, a detailed sketch, and lastly a simulation before a conclusion is reached.

### 1.1 Light Absorption in Semiconductors

The common absorber employed in solar cells is silicon. This material has an energy bandgap  $E_g=1.12\text{eV}$ , meaning an incoming photon must have at least 1.12eV of energy to free an electron from the valence band into the conduction band. All photons under this threshold do not free up electrons. Translating from energy to wavelength, this means any wavelength longer than 1130nm - assuming a refractive index of 1 - cannot be converted into electricity. As for photons with energy above this threshold, their excess energy is transferred into heat which is wasteful. The reader will see from **Figure 1** that this renders much of our incoming spectrum of sunlight as uncaptured, and still more as over-compensated:

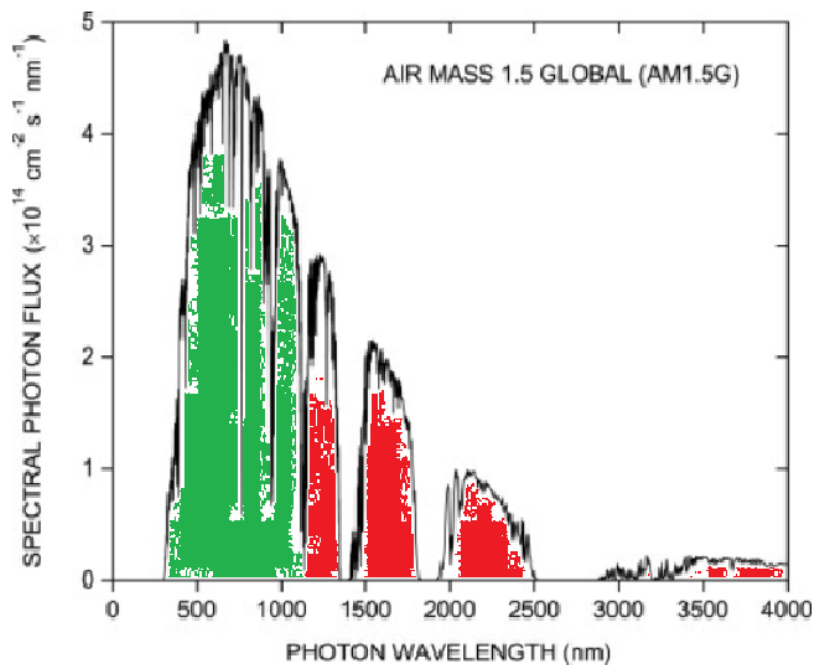


**Figure 1.** Solar energy spectra of impinging photons per  $\text{cm}^2$  per second in an air mass environment or AM of 1.5G – the typical air mass for Earth’s surface (modified from Kurnaiwan Fig 2). The green-filled region is the range of wavelengths convertible by Silicon which fits the scenarios of **Figure 2a & 2b**. The red-filled region are the wavelengths with insufficient energy for Silicon to convert which fits the scenario in **Figure 2c**.

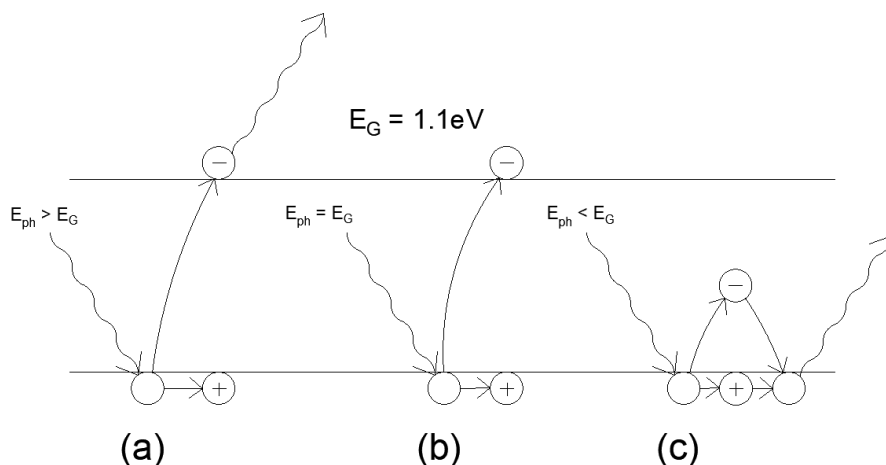


**Figure 2.** Scenarios for impinging photons on silicon: **(a)** Photon energy is significantly above bandgap. **(b)** Photon energy is sufficient for photoelectric effect. **(c)** Photon energy is insufficient for photoelectric effect

The solar spectrum ought to be more effectively utilized, and this can be done by adding another absorber with a higher bandgap than silicon, and placing it on top. Since a photovoltaic cell can be thought of as a light-absorbing diode - having a p-n junction - then solar cells stacked with additional absorbers can be referred to as multi-junction solar cells – having multiple p-n junctions. The top junction absorbs the higher energy photons a.k.a. shorter wavelengths. This frees electrons to the conduction band at an energy potential higher than if absorbed by some lower bandgap material. The higher energy potential can be outputted as higher current or higher voltage, depending on the load. As for any impinging photons of energy below the top semiconductor's bandgap, they will pass through the top junction and be absorbed by the underlying, lower bandgap junctions. When multiple junctions are in play, more of the solar spectrum can be converted into electricity and less heat excess is produced. Below is a simplified depiction of solar cells with incrementing amounts of p-n junctions:

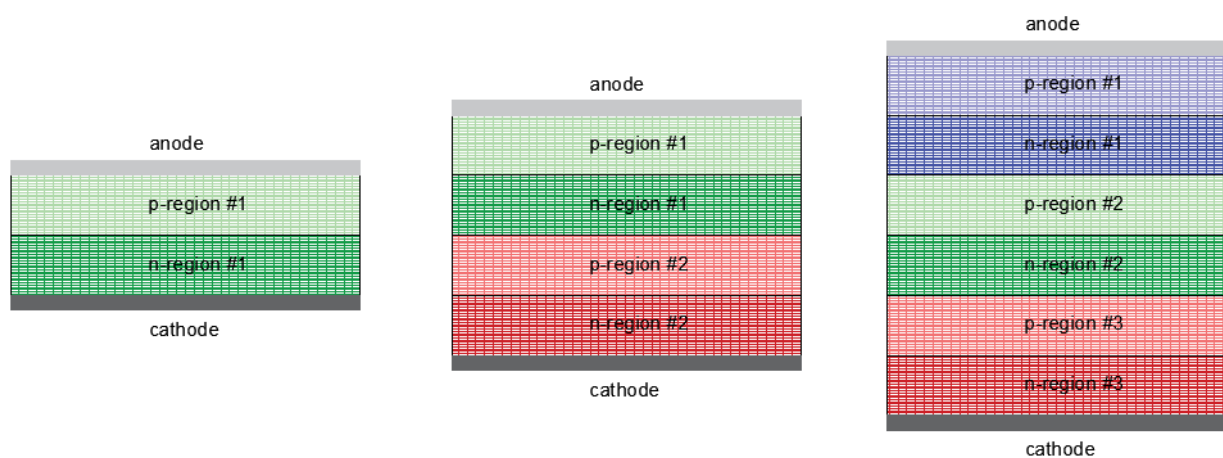


**Figure 3.** Simplified solar cells: single-junction (**left**), tandem or double-junction (**middle**), and triple-junction (**right**)

Thomas Dittrich's book *Material Concepts for Solar Cells* describes a significant increase in theoretical efficiency from single-to-double and double-to-triple junction solar cells as 32% → 44% and 44% → 50%. Quadruple junction solar cells have also been researched, which pushes the efficiency further from 50% → 54%. However, such a quadruple-junction design will have added costs, costs which I think will probably outweigh the marginal increase in efficiency. Furthermore, the realization of highly efficient quadruple-junction solar cells is still challenging in practice (Dittrich p199-200). For these reasons, a triple-junction solar cell is pursued instead.

Each of the junctions in the cell can be thought of as a current or voltage source depending on the context. If there are no intermediate contacts, as shown above in **Figure 3**, then the junctions are practically connected in series. In this context, they are modeled as voltage sources because voltage is being summed at the output. If, however, intermediate contacts were in place then the junctions could be arranged together in parallel and resemble current sources since current is being summed at the output. See **Figure 4**:

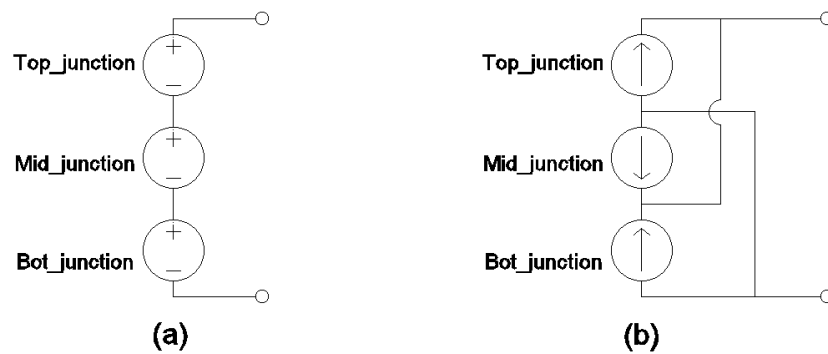


**Figure 4.** Equivalent circuit diagrams of (a): a triple-junction solar cell with no intermediate contacts, arranged in series; and (b): a triple-junction solar cell with intermediate contacts, which are then tied so that a parallel arrangement is achieved

Given that the research in multi-junction solar cells is saturated with series configurations, this thesis will pursue a parallel configuration to see how it differs. Perhaps more power output can be achieved.

Now whether in series or in parallel, the p-n junctions in a solar cell can end up working against each other, making them less effective. Before analyzing how this occurs in parallel arrangements, let's first analyze how this happens in a series configuration. (This will give background, to help us understand the obstacle facing parallel junctions.)

Whereas before we modeled the series configuration as voltage sources, now we will model them as current sources. With series current sources, the output current is only as strong as the weakest source. This is because in order to maintain the law of charge conservation, the current across a section of wire must be equal at all points. If the weaker sources cannot match the stronger current source, then the stronger source will shunt its surplus generated current through its internal shunt resistance. This results in heat loss – decreasing efficiency and reducing device lifetime due to thermal stress. See **Figure 5**:

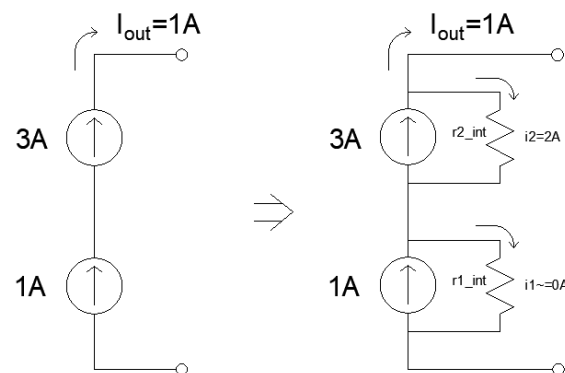


**Figure 5.** Equivalent circuit diagram of unequal current sources connected in series

This problem with series arrangements, called the current matching condition, is averted by balancing the currents via matching short-circuit current among the junctions.

In solar cells with parallel geometries, the problem is now directed towards voltage instead of current. Modeled as voltage sources, the configuration's output voltage is only as strong as its weakest junction or source. To understand why, remember the conservation of energy and how it implies Kirchoff's voltage law: that the sum of all the electric potential differences in a loop must equal zero - in order to return to the starting potential. So for loops involving only voltage sources, any voltage source which is stronger than its parallel-connected neighbor(s) will drop its excess voltage across its internal series resistance, which is heat loss. See **Figure 6**:

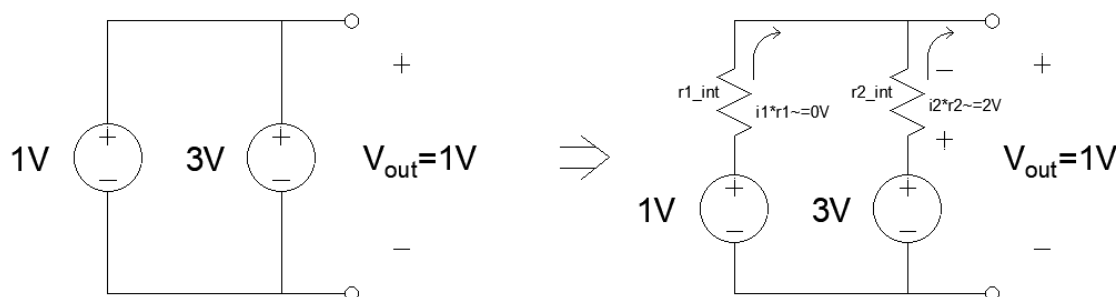


**Figure 6.** Equivalent circuit diagram of unequal voltage sources connected in parallel

Therefore, the voltages must be balanced, and doing this means matching the open-circuit voltage among the junctions, so how does one affect the open-circuit voltage? To explain how, and to be clear of confusion, let's first define some terms which the reader may be familiar with from experience with energy band diagrams:

*Fermi-level* – the energy level at which an electron has a 50% chance of filling some quantum state; can also be defined as the mean energy for electrons in some material

*workfunction* – the difference in energy between the vacuum level and Fermi-level for some material

*electron affinity* – the difference in energy between the conduction band and the vacuum level

*hole affinity* – the difference in energy between the valence band and the vacuum level.

We should also first cover the details of how a solar cell supplies current and voltage. Solar cells supply current by being able to generate electron-hole pairs from the photons it absorbs, separate those charges, then sending electrons towards cathode and holes towards the anode. The charge separating mechanism is [typically] the electric field which presides over the depletion region within the p-n junction. The voltage supplied by the solar cell depends on light exposure, cell efficiency, and the demands of the external circuit. If, say, the external circuit shorted the anode and cathode, then there would be no difference in electric potential between the electrodes and thus maximum or short-circuit current would be supplied. But if the external circuit was an open-circuit, then there would exist no current and the voltage across the anode and cathode would be at its maximum or open-circuit voltage. Seen from the energy band diagram in **Figure 7a-b**,

this electric potential between the contacts is equivalent to the splitting of the Fermi-levels between the p and n-regions. In the case of **Figure 7**, the most these Fermi-levels can be split a.k.a. the open-circuit voltage is limited by the difference in workfunction between the contacts a.k.a. the built-in voltage (**Equation 1**).

$$\text{Equation 1.} \quad V_{BI} = \phi_{cL} - \phi_{cR} \quad (\text{Fonash p73})$$

$V_{BI}$  – the built-in voltage

$\phi_{cL}$  – the contact workfunction on the left (or top)

$\phi_{cR}$  – the contact workfunction on the right (or bottom)

At the maximal degree of Fermi-level splitting (**Figure 7b**), the conduction and/or valence band has gone flat across the p-n junctions due to the load voltage cancelling the internal electric field, meaning charges can no longer be split and so no current exists. Any further Fermi-level splitting such as in **Figure 7c** – which would have to be done by some external source - would actually reverse the current and thus consume power rather than supply it.

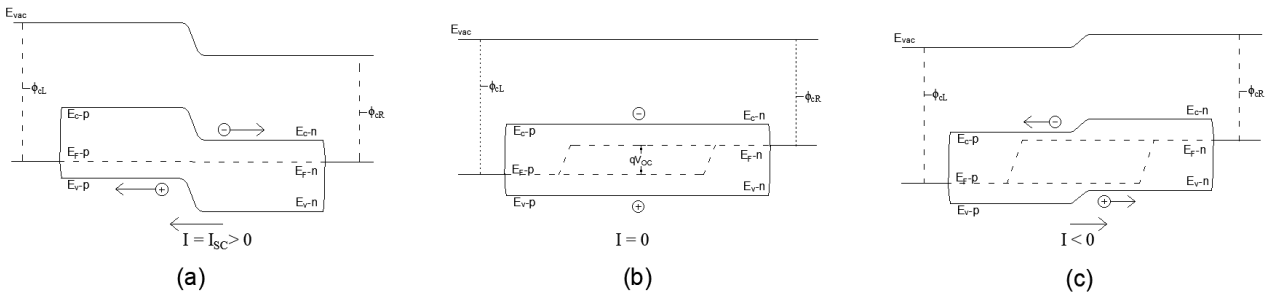


**Figure 7.** Band diagrams for an unspecified solar cell with varying amounts of Fermi-level splitting: **(a)** the Fermi-level splitting (or lack thereof) that occurs at short-circuit conditions, **(b)** the Fermi-level splitting at open-circuit conditions, and **(c)** the Fermi-level splitting for extreme forward bias (reversing current)

So perhaps the voltage for all three junctions can be balanced by doping the contacts. This way the difference in workfunction for all three junctions (at their contacts) will be nearly the same, and can be a very high value if given high doping. Yet, this idea cannot get off the ground because conductors are practically unaffected by doping. With insulators, doping fills either states in the conduction band with electrons or states in the valence band with holes that could not have been filled otherwise; but with conductors, the valence and conduction bands overlap, so the electrons and holes are already free to move about the bands from one state to another. Therefore, doping has little added effect on the likelihood of a state being filled: the Fermi-levels move very little.

Similar to the previous idea but even simpler: why not just find some pair of contact materials with a large built-in voltage and use this same pair for all three junctions? The built-in voltage could be as large as desired – as large as possible! However, this too won't work. Consider **Figure 8**, specifically parts **b-c**, where we have a set of contacts whose built-in voltage exceeds the bandgap. In this scenario, electrons are accumulated in the semiconductor near the cathode and

holes are accumulated in the semiconductor near the anode. This happens because electrons move from places with low workfunctions to places with high workfunctions in order to reach equilibrium. Likewise, holes move from places with high workfunctions to places with lower workfunctions. This resulting build-up of charge at the contacts creates an electric field which prevents holes from leaving the anode and electrons from leaving the cathode, so the cell reaches open-circuit conditions prematurely. The Fermi-levels are said to be “pinned”. Any further splitting could only be achieved by an outside source, sending an electric field through the cell to combat the built-up field, which would consume power. Hence, it is not profitable to have a pair of contacts whose built-in voltage is far greater than the bandgap.

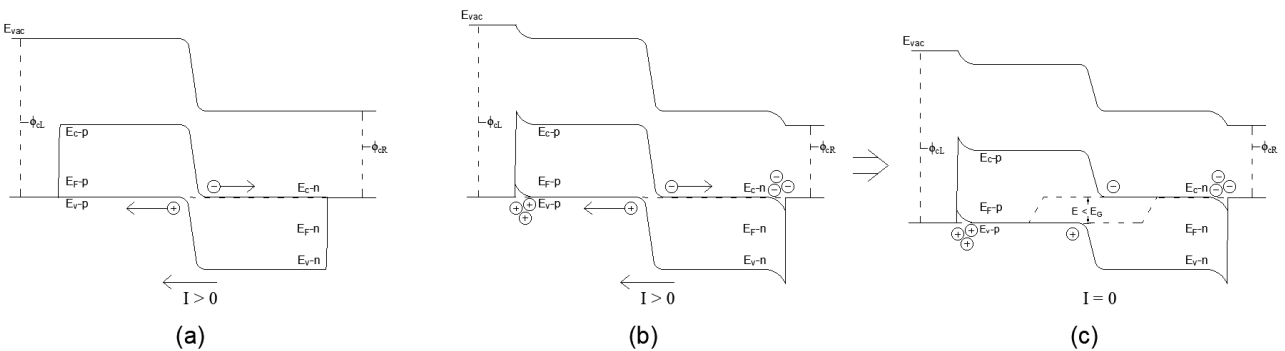


**Figure 8.** Band diagrams for an unspecified solar cell with extreme doping and highly disparate contact workfunctions. **(a):**  $\Delta\phi_c = E_G$  **(b):**  $\Delta\phi_c > E_G$  **(c):**  $\Delta\phi_c > E_G$  and at open-circuit conditions

There’s also the idea of doping the p and n-regions so that the Fermi level penetrates into the valence band and conduction band, respectively. In theory, this would allow for Fermi-level splitting that exceeds the bandgap (**Figure 9a**). Yet, such a high concentration in doping, called degenerate doping, would lead to a very thin energy barrier (and a very thin depletion region) - so thin, in fact, that the electrons in the n-region’s conduction band would recombine with holes from the p-region’s conduction band via quantum tunneling (**Figure 9b**). Additionally, the high concentration of impurities would greatly decrease the charge mobility. Thus, external voltage would increase at the cost of greatly diminishing external current. Still, in order to maximize the open-circuit voltage limit, while avoiding degenerate doping, it will be necessary to dope the regions to move the Fermi-level to within .08eV of their bands.

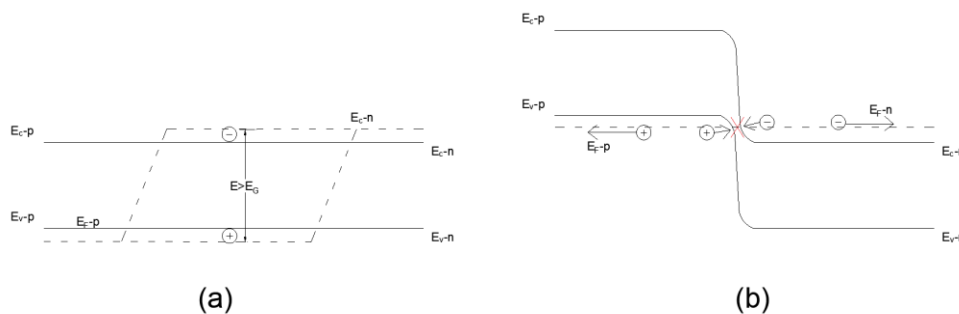


**Figure 9.** Band diagrams of a solar cell with degenerate doping **(a):** ideal diagram at open-circuit conditions **(b):** short-circuit conditions

With all of these scenarios in mind: doping the contacts, built-in voltage exceeding the bandgap, and degenerate doping - it can be justifiably said that the open-circuit voltage for a solar cell is less than or equal to the built-in voltage, and the built-in voltage is *practically* limited by the semiconductor bandgap (**Equation 2**).

$$\text{Equation 2.} \quad V_{OC} \leq V_{BI} \lesssim E_G \quad (\text{based on Fonash p82})$$

$V_{OC}$  – the open-circuit voltage

$E_G$  – the semiconductor bandgap

The reader will probably see by now the issue with trying to balance the voltages among different bandgap absorbers. Namely, the lower bandgap materials cannot match their open-circuit voltage with that of the upper, higher-bandgap junctions because of an intrinsic material property (the bandgap) that cannot be changed. At this point, any balancing of the voltages would look like doping the upper junctions to split the Fermi-levels only as far as the lowest bandgap material can manage, inhibiting the voltage output of the upper layers. This method would inhibit the current output, too. The short-circuit current and hence the I-V curve of a solar cell is affected by open-circuit voltage. As described in **Equations 3&4** and apparent in **Figure 10**, lowering the open-circuit voltage for these upper junctions would also lower the short-circuit current and hence the maximum power output.

$$\text{Equation 3.} \quad V_{OC} = \frac{k_B T}{q} \ln\left(\frac{I_{SC}}{I_0} + 1\right) \quad (\text{Dittrich p12})$$

$$\text{Equation 4.} \quad I_{SC} = I_0 \exp\left(\frac{qV_{OC}}{k_B T}\right) \quad (\text{Dittrich p13})$$

$k_B$  – Boltzmann's constant

$T$  – Temperature (300K)

$q$  – the charge of an electron

$I_{SC}$  – the short-circuit current

$I_0$  – the diode saturation current

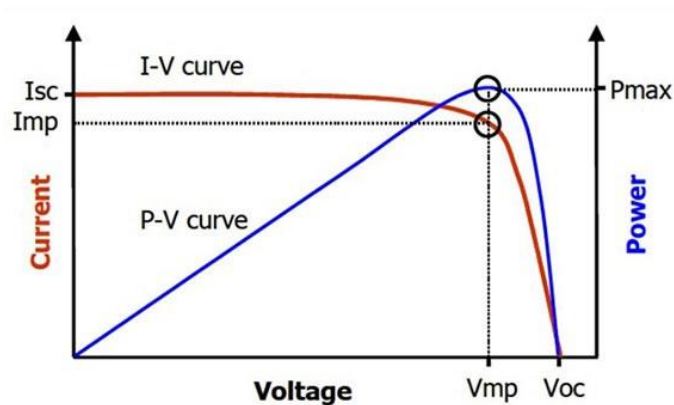


**Figure 10.** Simplified depiction of a I-V overlaid with a P-V curve for an unspecified solar cell (Schweber Fig 2).



The open-circuit voltage is limited by the built-in voltage, or at least with homojunctions. The same is not true for *heterojunctions*. (A heterojunction is made when the p-region and n-region are made of two different semiconductors. This is in contrast with the more commonly made homojunction, wherein the semiconductor is the same for both the p-region and n-region.) Research shows that the open-circuit voltage is not limited by the built-in voltage in heterojunctions (Fonash p188), and perhaps the  $V_{OC}$  for such heterojunctions is not limited by the bandgap, either. In which case, the  $V_{OC}$  of the lower junctions can be tailored to approximate the  $V_{OC}$  of the top junction by pairing the lower two bandgap absorbers with higher bandgap materials. The type of heterojunction I propose is an absorber-window type. A window does not absorb any photons due to its having a large bandgap. Instead, it is there primarily to separate charges at the interface where the window meets the absorber while contributing to the output voltage. In fact, a heterojunction without any doping can still create a voltage at the contacts. This voltage contribution is due to the window having a different electron and/or hole affinity than its mated absorber, whereby it splits charges across the interface by means of a step in affinity. This undoped interface, while not having an electric field, is still effective at splitting the charges and is thus said to have an “effective field.” Below are band diagrams of these two kinds of junction, one using only an electric field and another using only an effective field:

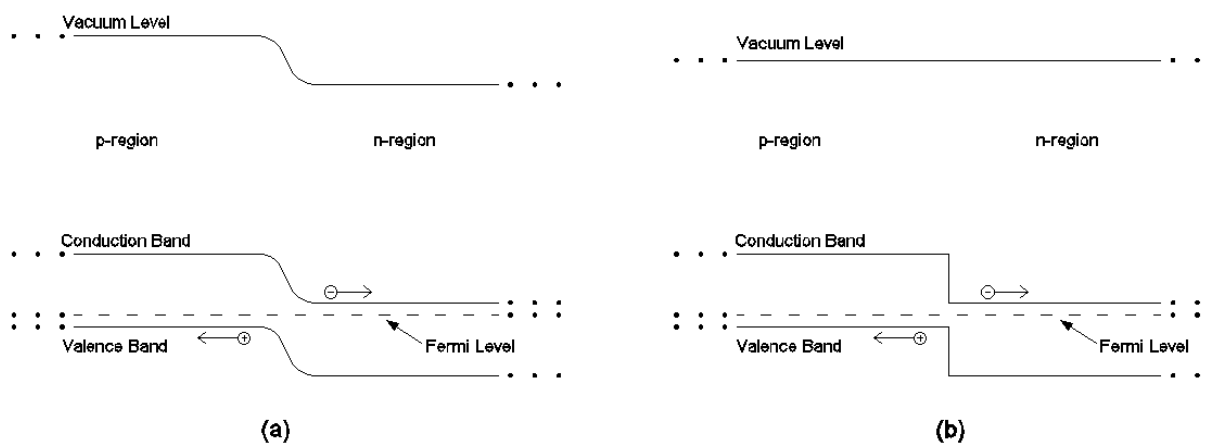


**Figure 11.** (a) A junction using only electric fields, created by doping, and (b) a junction utilizing only effective fields, created by differences in affinities (right).

By combining these two fields into one junction, involving a doped window, voltage and charge transport could be optimized.

The selected windows should have a bandgap too large to interfere with the photon absorption of its mated absorber, and ought to have a lattice constant close to that of its mate. If the lattice constants between the window and absorber can be approximately matched, then there will be no charge trapping and recombination at the interface. Another benefit of two crystals having the nearly the same lattice constant is that they can be grown one atop the other, which eases the manufacturing process.

## Chapter 2 : Design

There now lie multiple decisions to make for this multi-junction, parallel cell containing hetero-junctions: Which absorbers should be used for the junctions? Which windows? In the heterojunctions, should the absorber be p-type or n-type, and should it go on top of its mated window or be bottom?

Choosing the absorber materials depends on what bandgaps they have, as we want to choose a spread of three bandgaps that will maximize the amount of energy captured from the incoming photons, while dividing the photon spectrum into consecutive bandwidths that, when integrated the number of incoming photons, will equal one another. Take **Figure 12** for instance:

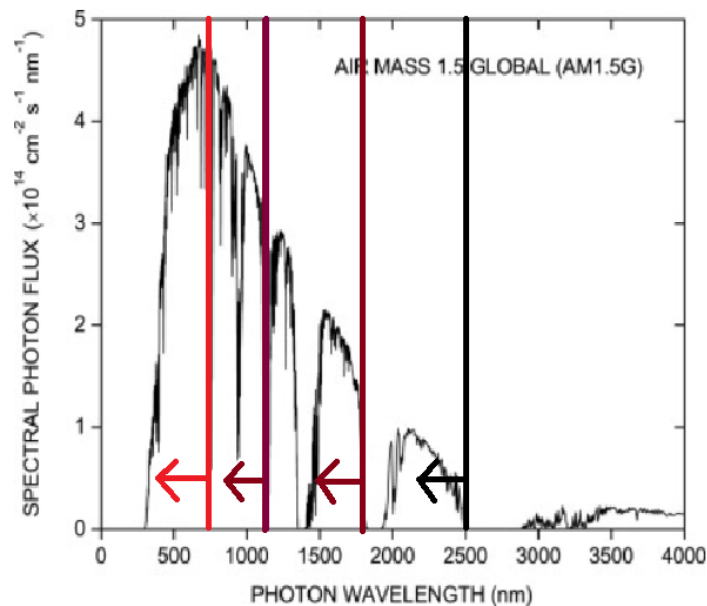


**Figure 12.** Solar spectrum of impinging photons in AM1.5G, with boundaries set to serve as limits for balanced consecutive integrals over the graph – not exact (modified from Kurnaiwan Fig 2).

The spread of bandgap energies will likely be in the lower range of available semiconductor bandgaps, which according to **Figure 13** promise the most short-circuit current density.

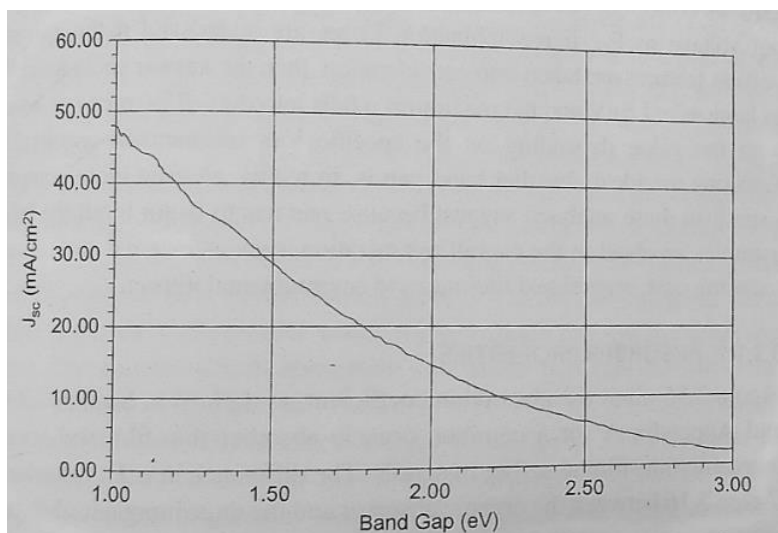


**Figure 13.** Potential short-circuit current density versus absorber bandgap for the AM1.5G spectrum (Fonash p95)

## 2.1 Material Selection

Research finds that the optimal bandgap distribution in a triple-junction cell is 0.7, 1.15, and 1.75eV. This has been tested using III-V semiconductors, reaching 36% efficiency (Dittrich p199). While these values may have been found most efficient only with respect to a series arrangement, nonetheless they still are the best proven bandgap spread. (On a tangent note: if a quadruple-junction cell were feasible, I would add a bandgap  $\sim 0.49$ eV to gather the last chunk of wavelengths from 2000-2500 nm as shown in **Figure 12**.) Since III-V semiconductors (crystal alloys coming from groups III and V in the periodic table) require special fabrication, we will look for more common crystals to approximate this optimal bandgap spread. In looking for alternative absorbers, there are single-crystalline, polycrystalline, and organic materials. So far in the literature and among colleagues, single-crystalline absorbers such as Silicon are reputed to be the most efficient kind (Fonash p189, Dittrich p199). I chose Germanium, Silicon, and Cadmium Selenide. Ge has a bandgap of 0.67eV; Si has a bandgap of 1.12eV; and CdSe has a bandgap of 1.68eV. All of these values are with respect to a temperature  $T=300$ K. Silicon and Germanium are the two most available semiconductors, and CdSe has been researched for some time now.

As we saw before, choosing the window materials revolved around two aims: the bandgap must be larger than - and the lattice constant must be close to - that of the paired absorber. GaP has a bandgap of 2.26eV and a lattice constant of 5.4505Å (angstroms), which pairs well with Silicon's lattice constant of 5.431Å. AlAs has a bandgap of 2.17eV and a lattice constant of 5.6608Å, which works well with Germanium's lattice constant of 5.658Å.

One of the major factors in deciding whether the absorber should be p-type or n-type and whether it goes top or bottom was the number of contacts required for any particular design choice.

For example, if the regions were arranged top-to-bottom as p-n – p-n – p-n then there would be 6 contact layers and 2 insulating layers between any “n – p” in order to keep the geometry parallel (**Figure 14a**). Without those insulating layers, the cathode of the top junction would be in direct contact with the anode of the mid-junction and likewise the mid-junction’s cathode would be in direct contact with the bottom-junction’s anode. The ‘parallel’ configuration would end up as a series configuration. If, however, the three junctions in parallel were layered so that the regions were p-n - n-p - p-n such as in **Figure 14b**, then there would only be 4 contact layers and 0 insulation layers required because an electrode would be shared between junctions. Similar to **Figure 14b** though not depicted, there is also the option of a top-to-bottom n-p – p-n – n-p geometry which will have the same benefit of reducing layer count.

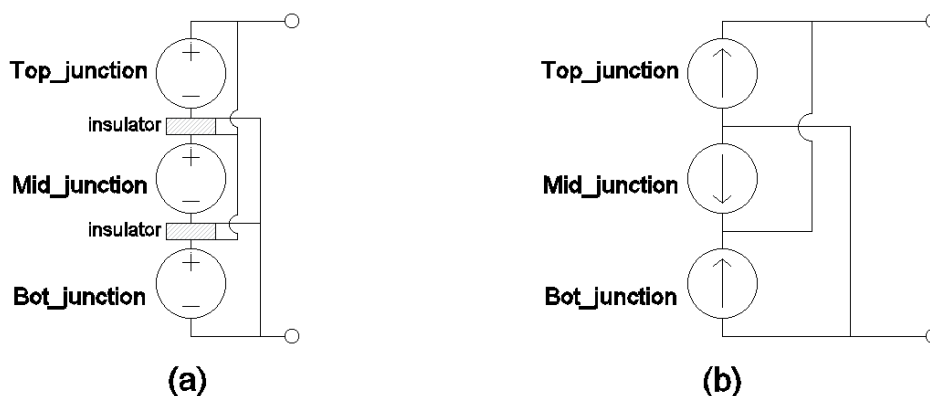


**Figure 14.** Two multijunction parallel cell geometries with contacts: (a) p-n – p-n – p-n structure with added insulating layers between the junctions (b) p-n – n-p – p-n structure with shared contacts between the junctions

For the top CdSe-CdSe layer, the only choice to be made was whether the p-region or n-region would be top. This will be heavily influenced by the comparison of diffusion lengths between electrons and holes. (Diffusion length is the distance a free charge carrier can traverse via diffusion transport before being lost by recombining with its counterpart.) To see why, consider the following: holes are either generated in the p-region or n-region. If generated in the n-region, they will have to diffuse to the depletion region, then drift across the entire p-region before being collected at the anode; if generated in the p-region, holes need only drift to the anode. Keeping this in mind, observe **Figure 15** which shows the additional number of absorbed photons exponentially decays with increasing distance from the surface of some semiconductor. Putting these two pieces of information together: if holes have the weaker diffusion length, then the p-region should be top. That way the majority of photogenerated holes need only drift a short distance before being collected at the anode. CdSe has a far weaker diffusion length for holes than for electrons, so it follows that the p-region should be incident to the light.

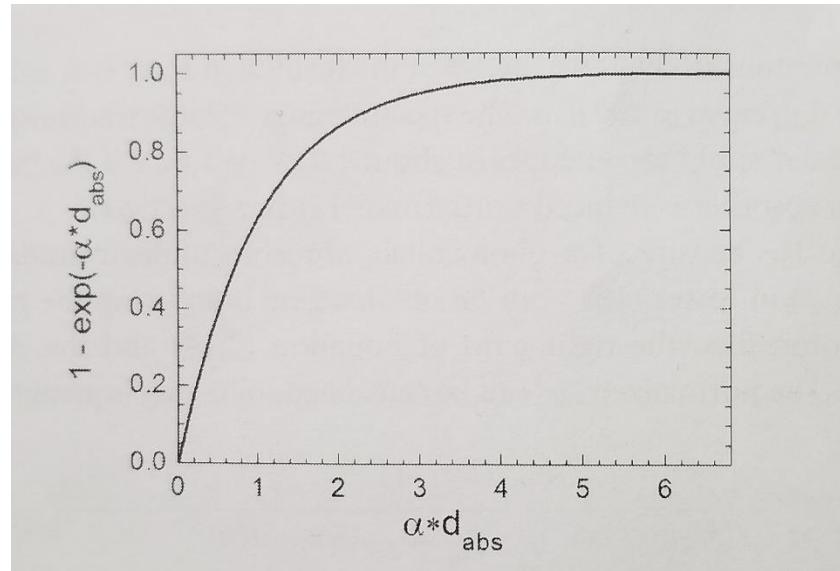


**Figure 15.** Number of absorbed photons as a function of the product of the absorption coefficient and the absorber depth. Exactly what is meant by the ‘absorption coefficient’ isn’t of importance here, only that photon absorption is related to absorber depth as a decaying asymptotic gain (Dittrich p55).

So then, with the p-region on top for the top junction, that means a p-n – n-p – p-n geometry is the ideal structure for minimizing the contact layer count. For further clarity, a simple sketch of this desired, ideal geometry is given below:

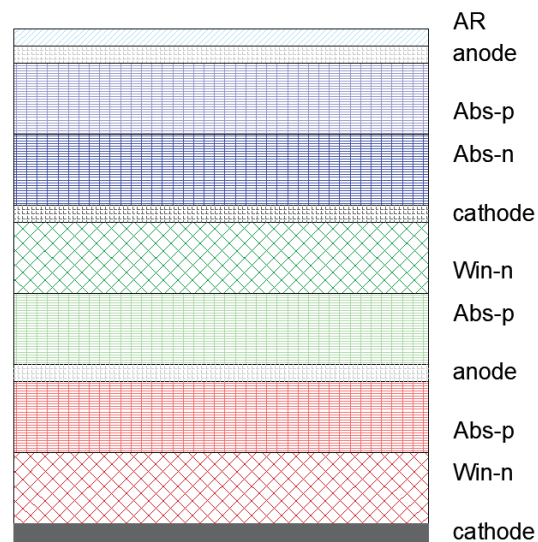


**Figure 16.** Simplified depiction of a solar cell with a p-n – n-p – p-n geometry

As for the lower absorber-window heterojunctions, where all of the light absorption and thus electron-hole pair generation occurs in the absorber, either the hole or electron will drift towards the contact on the absorber side, and its counterpart will diffuse to the depletion region

before drifting across the window to the opposite contact. The charge carrier that must make this longer trip ought to be the one that has the longer diffusion length.

Silicon has a higher diffusion length for electrons than for holes, and the window GaP has a higher electron diffusion length than hole diffusion length. Holes diffuse in the n-region and electrons diffuse in the p-region, so Silicon will be the p-region. Now it would be better for hole transportation if the Silicon p-region was incident to the light, placed atop the window, as it is with the CdSe layer - for the same reasons. But for the sake of maintaining the ideal geometry in **Figure 16**, I will place the p-region on the bottom. This compromise isn't so bad, since the hole diffusion length of Silicon isn't all that low. As for the lowest heterojunction, Germanium was made p-region for the same reasons Silicon was made p-region. To be more specific, Germanium and its partnered window, AlAs, both have higher electron diffusion lengths than hole diffusion lengths. And for this junction, in congruence with the desired geometry, the p-type can be incident to the light. As a side note, another good reason to have both of the absorbers -Silicon and Germanium - as p-type is that it permits exciton dissociation, which adds to the current. (Excitons are bound electron-hole pairs that must be dissociated at the heterojunction interface by the effective field (Fonash p114), and it is apparently necessary in an absorber-window heterojunction that the absorber be p-type for such a thing to occur (Fonash p238).)

Below is a table of all of the relevant material properties for the absorbers and windows used in the design. Some properties are particular to a certain wavelength, that wavelength being the approximate dominant wavelength for its junction bandwidth.

	<b>CdSe</b>	<b>GaP</b>	<b>Si</b>	<b>Ge</b>	<b>AlAs</b>
<b>Absorption Coefficient (cm<sup>-1</sup>)</b>	73,704 <sup>[4]</sup> ( $\lambda=600\text{nm}$ )	X	16.42 <sup>[4]</sup> ( $\lambda=1050\text{nm}$ )	453.24 <sup>[4]</sup> ( $\lambda=1600\text{nm}$ )	X
<b>Electron Diffusion Length (<math>\mu\text{m}</math>)</b>	$\leq 900$ <sup>[5]</sup>	$\sim 7$ <sup>[2]</sup>	50-1600 <sup>[2]</sup>	$\leq 3000$ <sup>[2]</sup>	?
<b>Hole Diffusion Length (<math>\mu\text{m}</math>)</b>	$\leq 137$ <sup>[5]</sup>	$\sim 20$ <sup>[2]</sup>	15-800 <sup>[2]</sup>	$\leq 2000$ <sup>[2]</sup>	?
<b>Bandgap (eV)</b>	1.68 <sup>[3]</sup>	2.26 <sup>[2]</sup>	1.12 <sup>[1]</sup>	0.67 <sup>[1]</sup>	2.17 <sup>[2]</sup>
<b>Electron Affinity (eV)</b>	4.7 <sup>[3]</sup>	3.8 <sup>[2]</sup>	4.05 <sup>[1]</sup>	4.0 <sup>[1]</sup>	3.5 <sup>[2]</sup>
<b>Intrinsic Effective Density of States in Conduction Band (cm<sup>-3</sup>)</b>	?	1.8E19 <sup>[2]</sup>	3.51E19 <sup>[1]</sup>	1.02E19 <sup>[1]</sup>	1.4956E19 <sup>[2]</sup>

<b>Intrinsic Effective Density of States in Valence Band (cm<sup>-3</sup>)</b>	?	1.9E19 <sup>[2]</sup>	1.87E19 <sup>[1]</sup>	5.64E18 <sup>[1]</sup>	1.6564E19 <sup>[2]</sup>
<b>Lattice Constant (Å)</b>	6.08 <sup>[5]</sup>	5.4505 <sup>[2]</sup>	5.431 <sup>[2]</sup>	5.658 <sup>[2]</sup>	5.6608 <sup>[2]</sup>
<b>Refractive Index</b>	2.624 <sup>[4]</sup> (λ=600nm)	3.1421 <sup>[4]</sup> (λ=1050nm)	3.568 <sup>[4]</sup> (λ=1050nm)	4.3031 <sup>[4]</sup> (λ=1600nm)	2.889 <sup>[4]</sup> (λ=1600nm)

*X – value is irrelevant*

*?-value is unknown*

**Table 1.** P-n junction material properties of the relevant to the solar cell design. Values were gotten either from: [1]-McNamara, [2]-Ioffe Institute, [3]-Royal Society of Chemistry, [4]-Poliyansky, or [5]-Springer within their contextual wavelengths and temperature T=300K

It needs to be mentioned that a material had to be chosen for an anti-reflective or AR layer, illustrated in **Figure 17**. The purpose of the AR layer is to soften the abrupt change in refractive index from the air to the substrate by having a refractive index value which is between the two - while being transparent. Doing this lessens the amount of light that will get reflected off of the surface of the solar cell. For finding which refractive index is desirable in the AR layer, the following equation helps:

**Equation 5.** 
$$n_{AR} = \sqrt{n_S * n_{air}} \quad (\text{Dittrich p52})$$

$n_{AR}$  – the desired refractive index of the AR layer

$n_S$  – the refractive index of the substance immediately beneath the AR layer a.k.a. ‘substrate’

$n_{air}$  – the refractive index of air: 1.003

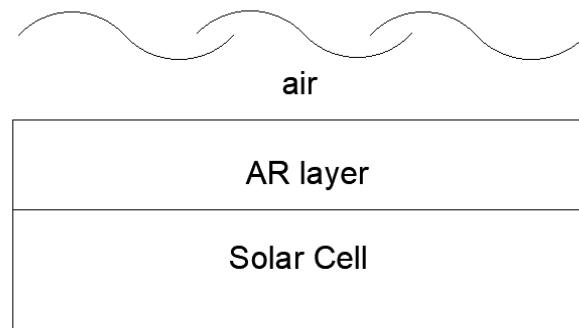


**Figure 17.** A basic illustration of an AR layer situated between the air and the solar cell

The crystal immediately below the AR layer for this design would be the top anode for which, as with all the contacts above the bottom contact, a Transparent Conducting Oxide or TCO was sought. TCOs are metal oxide compounds with a bandgap too large for the sun's rays to be absorbed, and can conduct electricity once given some amount of doping (they are one exception to the 'doping contacts is futile' prohibition I described earlier). Typically, the available TCOs are n-type meaning they are only good for cathodes, but new research has produced p-type TCOs from copper-based alloys which are not so technologically difficult to make (Stadler p4). As of 2009, CuBO<sub>2</sub> has proven a good room-temperature conductor with excellent transparency, where E<sub>g</sub>=3.2eV (Scanlon p1). A quality and easy to produce n-type TCO would be InO<sub>3</sub>[:Sn] of E<sub>g</sub>=3.3eV, which is quite common (Fonash p107). Without these TCOs, the contact layers would have to be some metal laid out in grid lines within an AR substrate. These grid lines would aim to block out the least amount of light from the below layers by being narrow while not being so narrow as to yield a high resistance. This would be disadvantageous compared to TCOs. The back contact, however, is best to remain non-transparent and even reflective. The reflectivity in the bottom contact effectively doubles the amount of layers light has to pass through in order to remain unabsorbed. Aluminum will do nicely since Aluminum is a very common, effective, and reflective conductor.

Relating this back to the AR layer: CuBO<sub>2</sub> has a refractive index of around 2.3 for a 600nm wavelength, and this resulted in a desired AR refractive index of:

$$n_{AR} = \sqrt{1.003 * 2.3} = 1.51885$$

Glass BK7 was chosen since it has a refractive index of 1.5161 and a high band gap of 4.21eV. For the relevant properties of the AR and conducting layers, see **Table 2**:

	<b>BK7</b>	<b>CuBO<sub>2</sub></b>	<b>InO<sub>3</sub></b>	<b>Al</b>
<b>Bandgap (eV)</b>	4.21 <sup>[1]</sup>	3.2 <sup>[2]</sup>	3.3 <sup>[3]</sup>	NA
<b>Refractive Index</b>	1.5161 <sup>[1]</sup> (λ=600nm)	2.3 <sup>[2]</sup> (λ=600nm) 1.8 <sup>[2]</sup> (λ=1600nm)	1.3636 <sup>[3]</sup> (λ=1050nm)	REFLECTS

**Table 2.** AR and conductor material properties of the relevant to the solar cell design. Values were gotten either from [1]-Joel, [2]-Scanlon, or [3]-Fonash within their contextual wavelengths and temperature T=300K

## 2.2 Doping Concentration and Layer Thickness Calculations

For any non-absorber material such as an anti-reflective layer, contact, or window, two factors were relevant for determining thickness: the minimum achievable length by non-esoteric manufacturing processes – which is ~10 μm, and which length would generate constructive



interference for the dominant incoming wavelength for that part of the cell. Aluminum, was the exception to the second concern since no light was expected to pass through. The AR layer should be made as thin as possible, since there is no benefit for added thickness. Windows should also be made as thin as possible, since any added thickness would only make the transport of carriers longer and therefore less successful. Contacts, on the other hand, should not be as thin as possible. As mentioned earlier, the thinner the contact is, the more resistance it will have, so a thickness above the minimum 10 $\mu$ m is advantageous. Further, the Aluminum layer needed to be somewhat thick to add sturdiness to the stack.

In addition to the above two concerns, any absorber material had its thickness determined by including considerations for the absorption and diffusion lengths. (Absorption length is the thickness of a material required in order to capture most absorbable light.) In all absorbers, being just above the absorption length parameter while being as far away as possible from the diffusion length parameter was the goal. In calculating thickness, **Table 1**, **Table 2**, and the following equations were instrumental:

**Equation 6.**  $\lambda = h \frac{c}{E}$

**Equation 7.**  $x = \frac{k\lambda}{2n} \geq 10\mu m$  (based on Dittrich p52)

**Equation 8.**  $k = \left\lceil \frac{2nx_d}{\lambda} \right\rceil$  (based on Dittrich p52)

**Equation 9.**  $x_{abs-p} + x_{abs-n} \geq 3L_{abs} = 3\alpha^{-1}$  (based on Dittrich p54)

**Equation 10.**  $L_{De/h} \geq x_{abs-p/n}$

$L_{De/h}$  – the diffusion length, for either electrons or holes

$x$  - the thickness of some layer:  $x_{abs-p/n}$  is for absorber p/n-region;  $x_d$  is the desired thickness

$L_{abs}$  – the length a material needs to be in order to absorb a photon, on average a.k.a. absorption length which is the inverse of the absorption coefficient  $\alpha$

$E$ – energy

$h$  – Planck's constant = 4.13567E-15 eV

$c$  – the speed of light=3E8 m/s

$\lambda$  – the wavelength

$k$  – a constant belonging to the set of natural numbers

$n$  – the refractive index of the layer

Calculating the doping depended on knowing what is the maximal open-circuit voltage for the CdSe homojunction, to be matched by the lower heterojunctions. We know this maximum is practically limited by CdSe's bandgap, and the closest we can approach this value is by shifting the Fermi levels to within .08eV of their respective region bands via doping. The open-circuit

voltage of the top junction, to be matched by the bottom junctions, is:  $1.68 - 2 \cdot 0.08 = 1.52\text{eV}$ . The following equations apply:

**Equation 11.**  $n_0 = N_C e^{\frac{E_C - E_F}{-k_B T}}$  (McNamara p22)

**Equation 12.**  $n_0 \cong N_D$  (McNamara p26)

**Equation 13.**  $p_0 = N_V e^{\frac{E_F - E_V}{-k_B T}}$  (McNamara p22)

**Equation 14.**  $p_0 \cong N_A$  (McNamara p26)

$n_0$  – the electron concentration

$p_0$  – the hole concentration

$E_C - E_F$  - energy difference between the conduction band and Fermi-level

$E_F - E_V$  - the energy difference between the Fermi-level and valence band

$N_C/V$  - the effective density of states in the conduction/valence band

$N_D/A$  - the doping concentration of donor/acceptor atoms

(In practice, none of the above equations could be used for CdSe since neither the effective density of states for the conduction band nor for the valence band could be found anywhere on the web.)

For the absorber-window heterojunctions, the calculated doping would be whatever non-degenerate amount brought the open-circuit voltage to 1.52V. Since we know doping the absorbers with impurities brings about defects which decrease diffusion and drift length, the lion's share of the doping should be in the windows. However, increasing the open-circuit voltage past the built-in voltage in a heterojunction does not appear to be an exact science. To my knowledge, there is no analytical set of equations to answer exactly *how* much doping is needed in order to match 1.52V. Rather, optimal doping levels would have to be approximately solved using numerical methods. In practice, this would mean running a simulation of incrementing doping concentrations for the absorber while the window is nearly (or fully) maxed-out.

### Parallel Triple-Junction, Using Heterojunctions

In what follows are the calculations for parallel triple-junction cell, involving heterojunctions. For each layer the thickness is solved for using **Equations 6-10**, then the maximum non-degenerate doping is found using **Equations 11-14** (only for the absorbers and windows). To see where all of the given constants/properties come from, please refer back to **Tables 1-2**. All final answers for thicknesses were rounded off to the nearest nanometer or third decimal place, and all final answers to the doping concentration were rounded off to the second decimal place.

Starting with BK7, we only care about having its thickness set so that reflected waves constructively interfere with the most prevalent wavelength for some subrange of the solar spectra. For the top layer, the whole range is available. Roughly estimating, it would seem from **Figure 1** (or **12**) that the most prevalent wavelengths focus around 600nm, so the thickness is calculated as:

$$BK7: \lambda = .6\mu m, n = 1.5161 \rightarrow x = \frac{.6k}{2 * 1.5161} = .197876k$$

$$x_d = 10\mu m \rightarrow k = \left\lceil \frac{10}{.197876} \right\rceil = 51 \quad \therefore x = .197876 * 51 = \mathbf{10.092\mu m}$$

Moving onto the topmost anode, made of  $CuBO_2$ , we won't set our desired length to the absolute minimum length of  $\sim 10\mu m$ , but instead let it be  $\sim 25\mu m$  for this as well as the other TCO layers for the sake of decreasing resistance. The calculations are:

$$CuBO_2: \lambda = .6\mu m, n = 2.3 \rightarrow x = \frac{.6k}{2 * 2.3} = .130435k$$

$$x_d = 25\mu m \rightarrow k = \left\lceil \frac{25}{.130435} \right\rceil = 192 \quad \therefore x = .130435 * 192 = \mathbf{25.044\mu m}$$

Again, the absorber layers have their diffusion and absorption lengths to account for in determining thickness.

Solving for CdSe:

$$CdSe: \alpha = 73,704cm^{-1} \rightarrow x_p + x_n \geq \frac{3}{73704} = .407\mu m$$

The length  $.407\mu m$  is too small to worry about given the total thickness over the p and n-regions has to be at least  $10\mu m$ .

$$L_{D_e} \leq 137\mu m, L_{D_n} \leq .09\mu m \rightarrow x_p \leq 137\mu m, x_n \leq .09\mu m$$

$$\lambda = .6\mu m, n = 2.624 \rightarrow x = \frac{.6k}{2 * 2.624} = .114329k \quad \therefore x_n = \mathbf{.114\mu m}$$

since this is the closest that  $.114329k$  can get to  $.09$

Setting the p-region thickness as far away from the hole diffusion length as possible,

$$x_{d-p} = 10 - x_n = 10 - .114 = 9.886\mu m \rightarrow k = \left\lceil \frac{9.886}{.114329} \right\rceil = 87$$

$$\therefore x_p = .114329 * 87 = \mathbf{9.947\mu m}$$

By design, doping would be set at the maximum for both regions, but due to previously mentioned concessions this had to be guessed as  $N_A = N_D = \mathbf{1.00E18cm^{-3}}$ .

The TCO cathode and the GaP-Silicon junction need to have calculated the wavelength they would aim to constructively interfere with. It is evident that CdSe would absorb all wavelengths under:

$$E_G = 1.68eV, \quad \lambda_G = \frac{hc}{E_G} = \frac{.0000012407}{1.68} = \mathbf{738.5nm}$$

**Figure 1** (or **12**) depicts that the most prevalent wavelengths past  $738.5nm$  cluster around roughly  $\sim 1050nm$ . (Once could argue for  $\sim 800nm$ , but that value is too close to  $600nm$ , and  $800nm$  will destructively interfere with wavelengths  $1.5 * 800 \cong 1200nm$  which has a high density according to the Figure.)

Solving for the upper cathode:

$$\text{InO}_3: \lambda = 1.05\mu\text{m}, n = 1.3636 \rightarrow x = \frac{1.05k}{2 * 1.3636} = .385010k$$

$$x_d = 25\mu\text{m} \rightarrow k = \left\lceil \frac{25}{.385010} \right\rceil = 65 \quad \therefore x = 65 * .385010 = \mathbf{25.026\mu\text{m}}$$

Solving for the thickness and maximum doping concentration of the upper window, GaP:

$$\text{GaP}: \lambda = 1.05\mu\text{m}, n = 3.1421 \rightarrow x = \frac{1.05k}{2 * 3.1421} = .167086k$$

$$x_d = 10\mu\text{m} \rightarrow k = \left\lceil \frac{10}{.167086} \right\rceil = 60 \quad \therefore x = 60 * .167086 = \mathbf{10.025\mu\text{m}}$$

$$N_C = 1.8\text{E}19\text{cm}^{-3}, E_{C-F} = .08\text{eV} \rightarrow N_D = 1.8\text{E}19e^{-\frac{.08}{.0259}} = \mathbf{8.20\text{E}17\text{cm}^{-3}}$$

Solving for Silicon:

$$\text{Si}: \alpha = 16.42\text{cm}^{-1} \rightarrow x_p \geq \frac{3}{16.42} = 1827.040\mu\text{m} \text{ and yet}$$

$$L_{D_e} = 1600 \text{ undoped} \rightarrow 1600\mu\text{m} \geq x_p$$

These two inequalities do not intersect, so one must take priority. It is more important that the thickness be narrow enough to allow charge collection than it is that it be wide enough to absorb all of the light, otherwise there is no output current. We can trust that at least the shorter wavelengths will be absorbed, and the longer wavelengths can be left for the bottom Germanium layer to collect. Therefore, let  $x_p = 1600$  minus the thickness for GaP since the electrons will have to move through that layer, too.

$$\lambda = 1.05\mu\text{m}, n = 3.568 \rightarrow x = \frac{1.05k}{2 * 3.568} = .147141k$$

$$x_d = 1600 - 10.025 = 1589.975\mu\text{m} \rightarrow k = \left\lceil \frac{1589.975}{.147141} \right\rceil = 10,805 \quad \therefore x = 10,805 * .147141 \\ = \mathbf{1589.859\mu\text{m}}$$

$$\text{Therefore: } N_A = \mathbf{0.00\text{cm}^{-3}}$$

Now that light has passed through both the CdSe and Silicon absorbers, all/most wavelengths shorter than:

$$E = 1.12\text{eV}, \quad \lambda = \frac{hc}{E} = \frac{.0000012407}{1.12} = \mathbf{1,108\text{nm}}$$

- have been absorbed. With Germanium as the last absorber, this only leaves wavelengths between 1,108nm and:

$$E = 0.67\text{eV}, \quad \lambda = \frac{hc}{E} = \frac{.0000012407}{.67} = \mathbf{1,852\text{nm}}$$

- of concern. Within this range, the most prevalent wavelengths center around 1600nm. With this value for wavelength, the lower anode's thickness will be calculated as:

$$CuBO_2: \lambda = 1.60\mu m, n = 1.8 \rightarrow x = \frac{1.6k}{2 * 1.8} = .444444k$$

$$x_d = 25\mu m \rightarrow k = \left\lceil \frac{25}{.444444} \right\rceil = 57 \quad \therefore x = 57 * .444444 = \mathbf{25.333\mu m}$$

Solving for Germanium:

$$Ge: \alpha = 453.24cm^{-1} \rightarrow x_p \geq \frac{3}{453.24} = 66.190\mu m$$

However, since the Germanium is almost adjacent to a reflective back contact, then the path of light is effectively doubled for this absorber. Thus  $x_p \geq \frac{66.19}{2} = 33.085\mu m$ .

$$L_{D_e} \leq 3000\mu m, L_{D_h} \leq 2000\mu m$$

Unlike in Silicon, the diffusion lengths are too large compared to the absorption length to be a limiter for either doping or layer thickness (since we try to stick just above the absorption length parameter).

$$\lambda = 1.60\mu m, n = 4.3031 \rightarrow x = \frac{1.6k}{2 * 4.3031} = .185912k$$

$$x_d = 33.085\mu m \rightarrow k = \left\lceil \frac{33.085}{.185912} \right\rceil = 178 \quad \therefore x = 178 * .185912 = \mathbf{33.092\mu m}$$

$$N_V = 5.64E18cm^{-3}, E_{F-V} = .08eV \rightarrow N_A = 5.64E18e^{-\frac{.08}{.0259}} = \mathbf{2.57E17cm^{-3}}$$

Solving for the thickness and maximum doping concentration of the lower window, AlAs:

$$AlAs: \lambda = 1.6\mu m, n = 2.889 \rightarrow x = \frac{1.6k}{2 * 2.889} = .276912k$$

$$x_d = 10\mu m \rightarrow k = \left\lceil \frac{10}{.276912} \right\rceil = 37 \quad \therefore x = 37 * .276912 = \mathbf{10.246\mu m}$$

$$N_C = 1.4956E19cm^{-3}, E_{C-F} = .08eV \rightarrow N_D = 1.4956E19e^{-\frac{.08}{.0259}} = \mathbf{6.81E17cm^{-3}}$$

Lastly, we'll set the bottom Aluminum contact as equal to 100μm.

### Parallel Triple-Homojunction

Thickness and doping values have to be solved again for a Silicon p-n homojunction so that I can compare my design against a similar parallel triple-junction design that doesn't use windows. In a Silicon homojunction, the addition of a Silicon n-region allows for the absorption length requirement to be shifted away from solely the p-region. That means the ~1800μm absorption length parameter can be fulfilled by summing the thicknesses of the p-region and n-region together, while each of those regions will be under their respective diffusion length. This means we can now dope the regions, increasing output voltage in a rival cell design. Using **Figure 18**, we can find such a pairing of diffusion lengths where:  $L_{D_e} + L_{D_h} \cong 3L_{abs}$  and then figure out (pun-intended) what doping is permitted for such lengths. When picking which pair of diffusion

lengths to use, I will make sure that the n-region is shorter than the p-region, since holes don't diffuse as well as electrons do in Silicon.

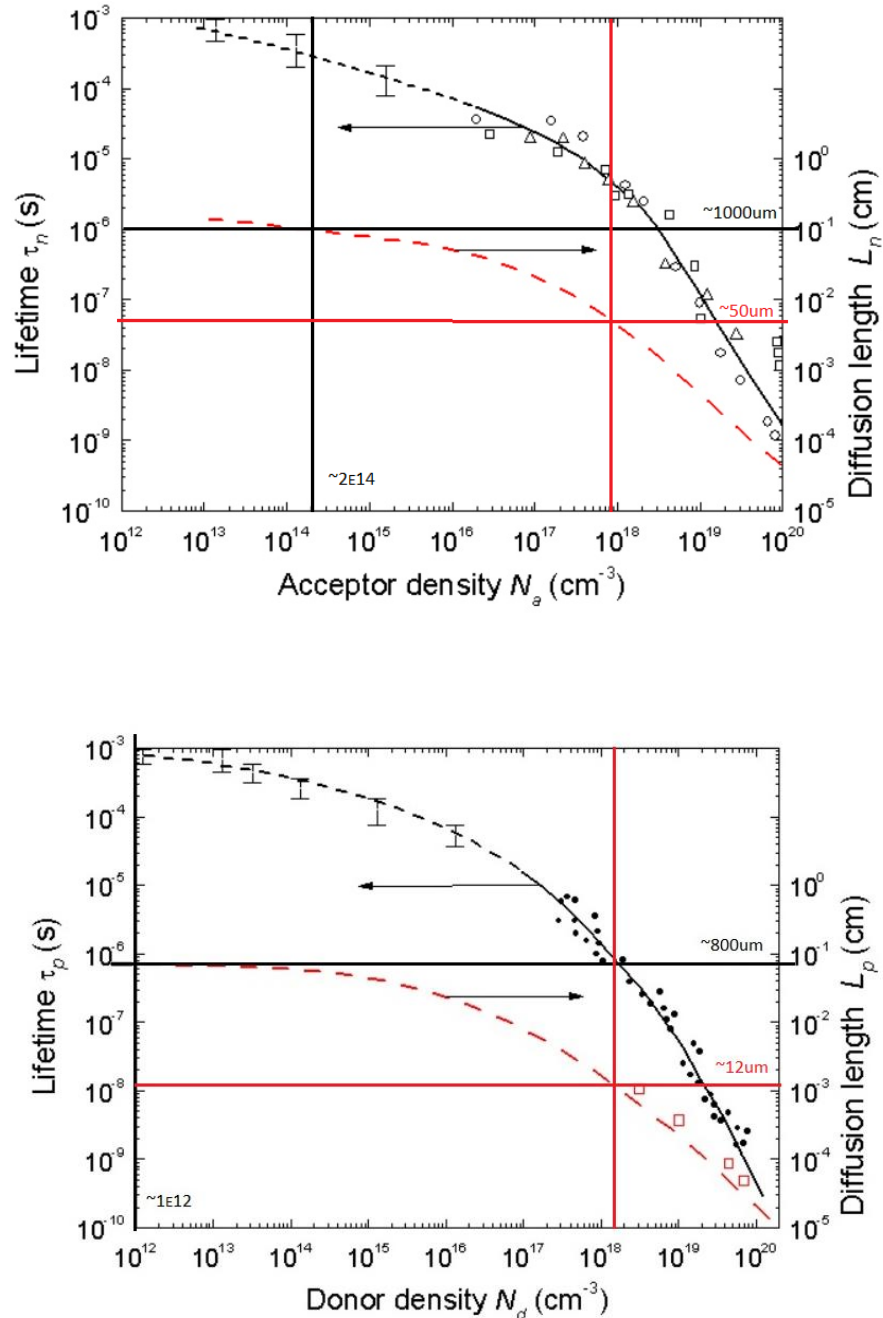


**Figure 18.** Diffusion length in Silicon vs Doping density for acceptors (**top**) and donors (**bottom**), provided by the Ioffe Institute. **Black** crosshairs are marked over the points on the curves where, when the diffusion lengths are summed together, the aforementioned absorption length requirement is satisfied in near-full. **Red** crosshairs are marked over the

points on the curve where the maximum n-type or p-type doping intersects with its correlated diffusion length.

From **Figure 18**, we can gather the doping and thicknesses are:

$$Si: N_A \cong 2.00E14cm^{-3} \text{ and } N_D \cong 1.00E12cm^{-3} \rightarrow x_{d-p} \sim 1000, x_{d-n} \sim 800$$

$$x_{d-p} \sim 1000 \rightarrow k_p = \left[ \frac{1000}{.147141} \right] = 6796 \quad \therefore x_p = 6796 * .147141 = 999.970\mu m$$

$$x_{d-n} \sim 800 \rightarrow k_n = \left[ \frac{800}{.147141} \right] = 5436 \quad \therefore x_n = 5436 * .147141 = 799.858\mu m$$

Re-solving the Germanium layer for a windowless homojunction, the doping ranges will be at the non-degenerate maximum as before, but the thicknesses will be in proportion to the diffusion lengths.

$$Ge: x_{d-p} = 33.092 * \frac{3000}{3000+2000} = 19.8552\mu m \rightarrow k = \left[ \frac{19.8552}{.185912} \right] = 107$$

$$\therefore x_p = 107 * .185912 = 19.893\mu m$$

$$x_{d-n} = 33.092 * \frac{2000}{2000 + 3000} = 13.237\mu m \rightarrow k = \left[ \frac{13.237}{.185912} \right] = 72$$

$$\therefore x_n = 72 * .185912 = 13.386\mu m$$

$$N_A = 2.57E17cm^{-3}; N_C = 1.02E19cm^{-3}, E_{C-F} = .08eV$$

$$\rightarrow N_D = 1.02E19e^{-\frac{.08}{.0259}} = 4.65E17cm^{-3}$$

### Series Triple-Homojunction

To compete against the parallel geometry, a series arrangement will be calculated for and simulated. In a series design, the doping for the Si junction will be non-degenerately maximized in order to raise the output voltage. Doing so will weaken charge transport across silicon, but this is tolerable because the role of the Si junction in a series arrangement is to maximize voltage. Afterall, any charges the Si generates would hardly reach the contacts, if at all, due to added mediums between it and the nearest contact. Generated charges in the Si also face inter-junction recombination. This inter-junction recombination is akin to the kind depicted in **Figure 9**, except it happens across the n-region of some p-n junction above with the p-region of the next p-n junction below, as shown here:

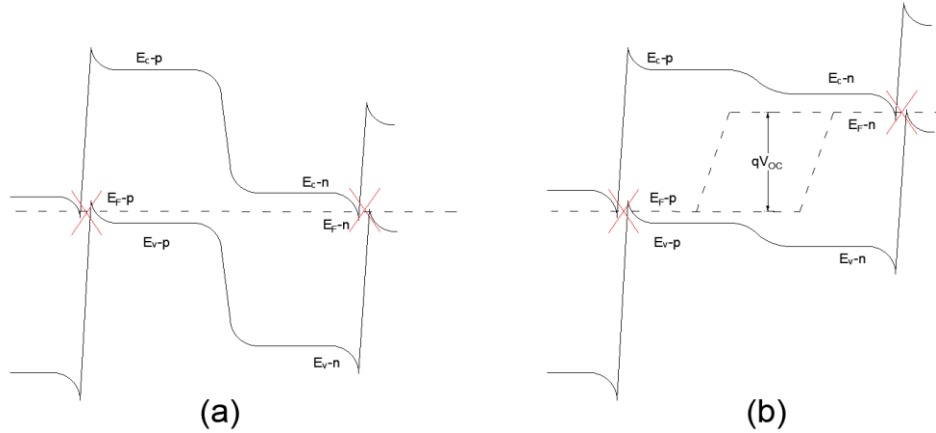


**Figure 19.** Band diagram segment of a series-arranged triple-junction solar cell operating at (a) short-circuit conditions, and (b) open-circuit conditions. Recombination sites are in red Xs.

So long as the current output of the Si junction in a series arrangement isn't so weak as to drag down the current output of the other junctions, then loss of charge mobility is okay. To watch for this, the thicknesses of the p and n-regions will be shortened as much as possible while keeping the doping at its peak. Doing so will ignore the absorption length parameter, but this too is acceptable since we want to leave more light for the bottom Germanium junction to absorb, that way the current from the bottom-junction is balanced with the others.

Solving again for Silicon, in the series arrangement, the maximum doping is:

$$Si: N_V = 1.87E19cm^{-3}, E_{F-V} = .08eV \rightarrow N_A = 1.87E19e^{\frac{.08}{-.0259}} = \mathbf{8.52E17cm^{-3}}$$

$$N_C = 3.51E19cm^{-3}, E_{C-F} = .08eV \rightarrow N_D = 3.51E19e^{\frac{.08}{-.0259}} = \mathbf{1.60E18cm^{-3}}$$

-and referring back to **Figure 18**, the lengths for the p-region and n-region are:

$$x_{d-p} = 50\mu m \rightarrow k = \left\lfloor \frac{50}{.147141} \right\rfloor = 339 \quad \therefore x_p = 339 * .147141 = \mathbf{49.881\mu m}$$

$$x_{d-n} = 12\mu m \rightarrow k = \left\lfloor \frac{12}{.147141} \right\rfloor = 81 \quad \therefore x_n = 81 * .147141 = \mathbf{11.918\mu m}$$

### 2.3 Desired Contact Workfunction Calculations

With the doping concentrations set, we can now imagine what the ideal workfunctions would be for the anodes and cathodes – to be used in the simulations. I am using the following equations. The given values are from **Tables 1 & 2** and the previous calculations:

**Equation 15.**  $\phi_S = E_{C-F} + X = (E_G - E_{F-V}) + X$

**Equation 16.**  $\phi_{WM} \geq \phi_{Wp}$  (Fonash p104)

**Equation 17.**  $\phi_{WM} \leq \phi_{Wn}$  (Fonash p104)



**Equation 18.**  $E_{C-F} = -k_B T \ln\left(\frac{N_D}{N_C}\right)$

**Equation 19.**  $E_{F-V} = -k_B T \ln\left(\frac{N_A}{N_V}\right)$

$\phi_S$  – the workfunction for a semiconductor

$X$  – the electron affinity

$\phi_{WM}$  – the workfunction for a metal

$\phi_{Wp}$  – the workfunction for the p-type semiconductor

$\phi_{Wn}$  – the workfunction for the n-type semiconductor

### Parallel Triple-Junction, Using Heterojunctions

*Top Anode (CuBO<sub>2</sub>):*  $\phi_{WM} \geq \phi_{W_{CdSe-p}} = (E_{G_{CdSe}} - E_{F-V_{CdSe-p}}) + X_{CdSe} = 1.68 - .08 + 4.7$   
 $= \mathbf{6.3eV}$

*Upper Cathode (InO<sub>3</sub>):*  $\phi_{WM} \leq \min(\phi_{W_{CdSe-n}}, \phi_{W_{GaP}})$

$$\phi_{W_{CdSe-n}} = E_{C-F_{CdSe-n}} + X_{CdSe} = .08 + 4.7 = 4.78eV ,$$

$$\phi_{W_{GaP}} = E_{C-F_{GaP}} + X_{GaP} = .08 + 3.8 = 3.88eV \quad \therefore \phi_{WM} \leq \mathbf{3.88eV}$$

*Lower Anode (CuBO<sub>2</sub>):*  $\phi_{WM} \geq \max(\phi_{W_{Si}}, \phi_{W_{Ge}})$

$$\phi_{W_{Si}} = (E_{G_{Si}} - E_{F-V_{Si}}) + X_{Si} = 1.12 - .56 + 4.05 = 4.61eV ,$$

$$\phi_{W_{Ge}} = (E_{G_{Ge}} - E_{F-V_{Ge}}) + X_{Ge} = .67 - .08 + 4.0 = 4.59eV \quad \therefore \phi_{WM} \geq \mathbf{4.61eV}$$

*Bottom Cathode (Alum.):*  $\phi_{WM} \leq \phi_{W_{AlAs}} = E_{C-F_{AlAs}} + X_{AlAs} = .08 + 3.5 = \mathbf{3.58eV}$

### Parallel Triple-Homojunction

Re-solving some of the contacts for a design that does not use windows:

*Upper Cathode (InO<sub>3</sub>):*  $\phi_{WM} \leq \min(\phi_{W_{CdSe-n}}, \phi_{W_{Si-n}})$

$$\phi_{W_{CdSe-n}} = E_{C-F_{CdSe-n}} + X_{CdSe} = .08 + 4.7 = 4.78eV ,$$

$$\phi_{W_{Si-n}} = E_{C-F_{Si-n}} + X_{Si-n}$$

$$E_{C-F_{Si-n}} = -k_B T \ln\left(\frac{N_D}{N_C}\right) = -.0259 * \ln\left(\frac{1E12}{3.51E19}\right) = .45eV$$

$$\rightarrow \phi_{W_{Si-n}} = .45 + 3.8 = 4.25eV \quad \therefore \phi_{WM} \leq \mathbf{4.25eV}$$

*Lower Anode (CuBO<sub>2</sub>):*  $\phi_{WM} \geq \max(\phi_{W_{Si-p}}, \phi_{W_{Ge-p}})$

$$\phi_{W_{Si-p}} = (E_{G_{Si-p}} - E_{F-V_{Si-p}}) + X_{Si-p}$$

$$E_{F-V} = -k_B T \ln\left(\frac{N_A}{N_V}\right) = -.0259 * \ln\left(\frac{2E14}{1.87E19}\right) = .30eV$$

$$\rightarrow \phi_{W_{Si-p}} = 1.12 - .30 + 4.05 = 4.87eV ,$$

$$\phi_{W_{Ge-p}} = (E_{G_{Ge-p}} - E_{F-V_{Ge-p}}) + X_{Ge-p} = .67 - .08 + 4.0 = 4.59eV \quad \therefore \phi_{WM} \geq \mathbf{4.87eV}$$

$$\text{Bottom Cathode (Alum.): } \phi_{WM} \leq \phi_{W_{Ge-n}} = E_{C-F_{Ge}} + X_{Ge} = .08 + 4.0 = \mathbf{4.08eV}$$

### Series Triple-Homojunction

The workfunctions for a series triple-junction will be the same as the top anode in the heterojunction design, and the bottom cathode in the homojunction design.

All of the values just solved for - thickness, doping, and workfunction – are summarized in **Table 3** below:

	Parallel Triple-Junction, with heterojunctions	Parallel Triple-Homojunction	Series Triple-Homojunction
BK7	$x_d = 10.092\mu m$	$x_d = 10.092\mu m$	$x_d = 10.092\mu m$
CuBO <sub>2</sub> - upper	$x_d = 25.044\mu m$ $\phi_{WM} = 6.3eV$	$x_d = 25.044\mu m$ $\phi_{WM} = 6.3eV$	$x_d = 25.044\mu m$ $\phi_{WM} = 6.3eV$
CdSe	$x_p = 9.947\mu m$ $x_n = .114\mu m$ $N_A = N_D$ $= 1.00E18cm^{-3}$	$x_p = 9.947\mu m$ $x_n = .114\mu m$ $N_A = N_D$ $= 1.00E18cm^{-3}$	$x_p = 9.947\mu m$ $x_n = .114\mu m$ $N_A = N_D$ $= 1.00E18cm^{-3}$
InO <sub>3</sub>	$x_d = 25.026\mu m$ $\phi_{WM} = 3.88eV$	$x_d = 25.026\mu m$ $\phi_{WM} = 4.25eV$	NA
GaP	$x_d = 10.025\mu m$ $N_D = 8.20E17cm^{-3}$	NA	NA
Si	$x_d = 1589.859\mu m$ $N_A = 0.00cm^{-3}$	$x_p = 999.970\mu m$ $x_n = 799.858\mu m$ $N_A \cong 2.00E14cm^{-3}$ $N_D \cong 1.00E12cm^{-3}$	$x_p = 49.881\mu m$ $x_n = 11.918\mu m$ $N_A = 8.52E17cm^{-3}$ $N_D = 1.60E18cm^{-3}$
CuBO <sub>2</sub> - lower	$x_d = 25.333\mu m$ $\phi_{WM} = 4.61eV$	$x_d = 25.333\mu m$ $\phi_{WM} = 4.87eV$	NA
Ge	$x_d = 33.092\mu m$ $N_A = 2.57E17cm^{-3}$	$x_p = 19.893\mu m$ $x_n = 13.386\mu m$ $N_A = 2.57E17cm^{-3}$ $N_D = 4.65E17cm^{-3}$	$x_p = 19.893\mu m$ $x_n = 13.386\mu m$ $N_A = 2.57E17cm^{-3}$ $N_D = 4.65E17cm^{-3}$
AlAs	$x_d = 10.246\mu m$ $N_D = 6.81E17cm^{-3}$	NA	NA
Al	$x_d = 100\mu m$ $\phi_{WM} = 3.58eV$	$x_d = 100\mu m$ $\phi_{WM} = 4.08eV$	$x_d = 100\mu m$ $\phi_{WM} = 4.08eV$

**Table 3.** Calculated values for each material (first column) relative to how it fits in a particular design (top row)

## Elaboration

Before simulations are run, it would be good to visualize my design in detail:

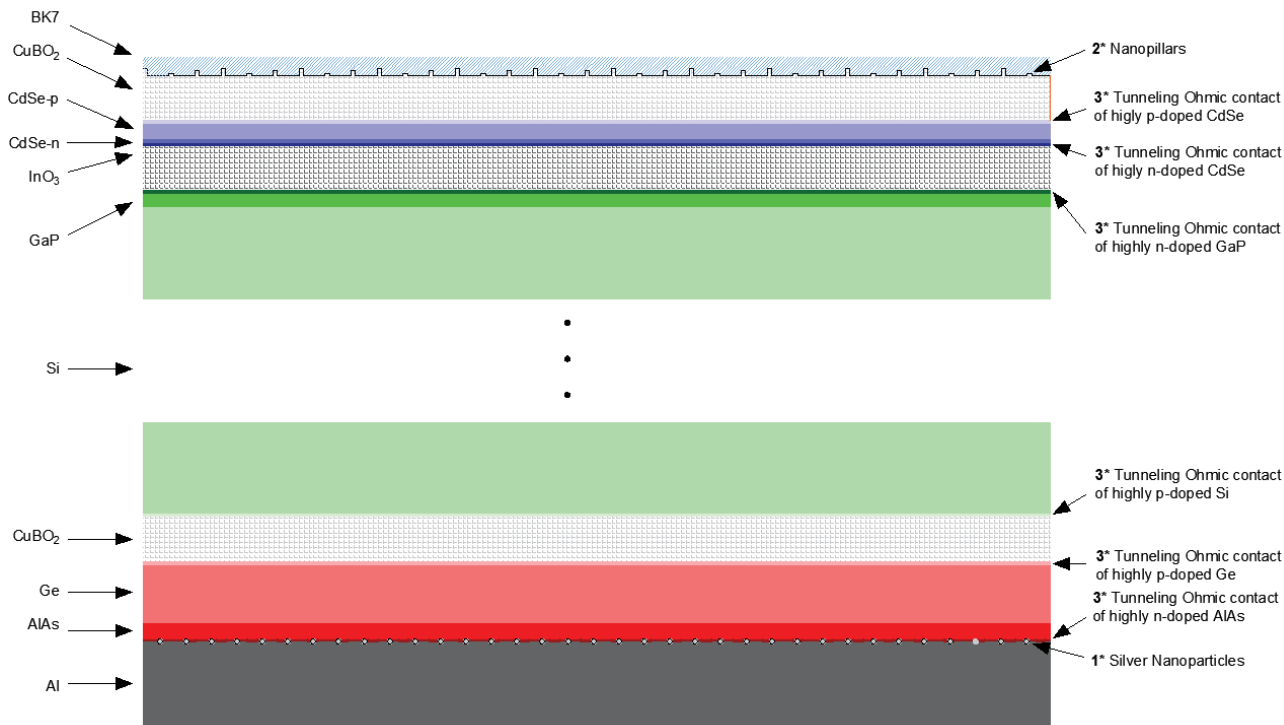


**Figure 20.** A sketch of the full design, mostly drawn to scale.

Marked in ' $n^*$ ' where  $n$  is some number, are features not mentioned before but are present for the sake of spreading the awareness of others' research. Feature '1\*' is the addition of silver nanoparticles of 100nm radius with a  $\sim 750$ nm lattice pitch placed at the back contact. This will enhance long wavelength absorption (Fonash p36). It works by employing cooperative electron oscillations, quantized into "plasmons". Plasmons originate from photons striking and scattering off of the electrons on nanoscale metal features. Once these plasmons have been set off, very strong near fields – short-range fields with high fluctuations in their electric and magnetic components - rise in which light absorption is enhanced. Silver was chosen since it resonates with waves that are roughly equal to or are a multiple of 390nm i.e. 780, 1170, 1560 & 1950nm, which covers a wide array of wavelengths that will remain once light reaches the bottom junction. Since silver is a great conductor, it is fitting to have it near/touching the Aluminum back contact. Feature '2\*' is the forming of the top surface of the contact, just beneath the anti-reflective layer, into nanopillars which help further to trap light within the cell. Coming from Fonash's book (page 34), nanopillars of  $\sim 25$ nm in radius, 0-231nm in height, and 150nm in center-to-center spacing provide adequate improvement to light-trapping. Feature '3\*' is the creation of tunneling contacts via highly doping the absorber/window near the contact. This region of high doping should be extremely thin, being less than a few nanometers, and saturated enough to move the Fermi level within the valence or

conduction band for the p or n-region, respectively. This creates a very thin energy barrier through which carriers will tunnel from the semiconductor into the contact. The thinner the barrier, the more probable the tunneling, but the more doping required. Tunneling contacts are decisive in solar cells with very high efficiencies (Dittrich 147).

The band diagram of a parallel arrangement, combining electric and effective fields with the inclusion of highly-doped tunneling layers, would resemble the following drawing:

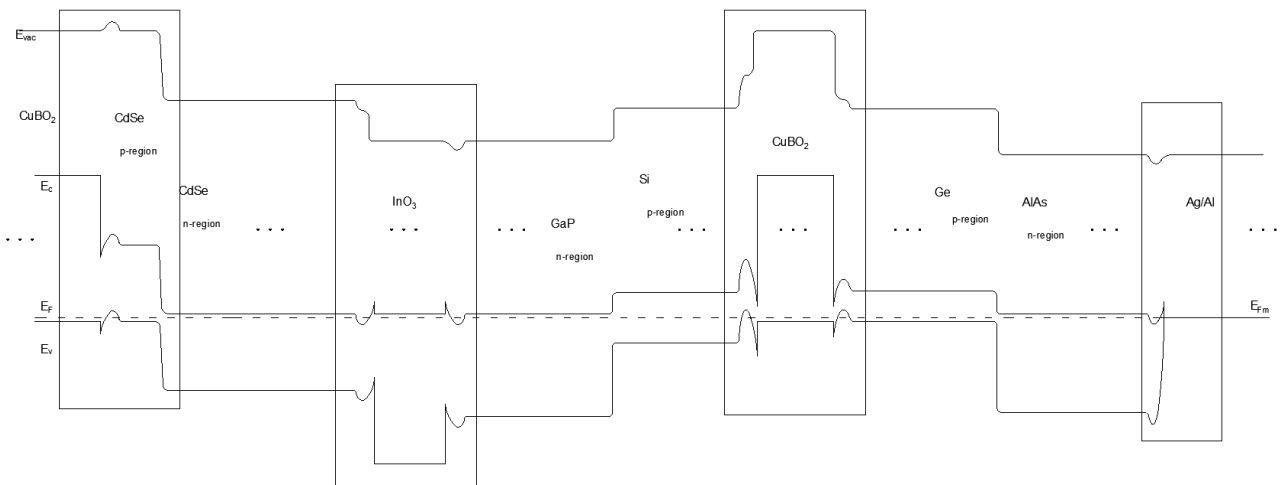


**Figure 21.** Approximate band diagram of entire cell design in short-circuit conditions, moving top-to-bottom as the drawing goes left-to-right. The vertical spacing is accurate, but the horizontal spacing is exaggerated at some parts to expand the tunneling contacts.

## Results

Using TCAD software, simulations were done of some cell designs based off of the previous suggestions. These designs were not as robust as the one given in the Elaboration, but they capture the core ideas of my research. My model assumes there to be perfect transparency of light waves through the conducting layers except for the bottom layer, a temperature of 300K, a typical solar irradiance at an air mass of AM1.5, and zero resistance in the conducting layers. (I can dream, can't I?) Other parameters, such as the doping amount chosen for CdSe, may not produce the optimal performance but are allowable since the key purpose of these simulations is to find the output *difference – ceteris paribus* - between designs so that a broad concept can be proven. Given this minimalist goal, this would allow the comparing of multijunction cells that have very poor performances so long as the cells vary in as few design features as possible. This way, the suspects for any difference in output among cell designs is narrowed down to just the design choice of interest. For the following simulations, all code can be found in the Appendix.

### Homojunction vs Heterojunction

The first two designs compared against one another is that of a single-homojunction Si solar cell versus a single-heterojunction solar cell with an Si absorber and a GaP window. There weren't any calculations in these two designs. The thickness was arbitrarily set and kept equal among the rival absorber layers so that the absorbed light should be about the same. The doping for both cells was non-degenerately maximized. Such inexactness is permissible since what we are looking for is merely whether or not adding a window layer can increase the output voltage as well as power for some cell. Below are the results for the homojunction cell:

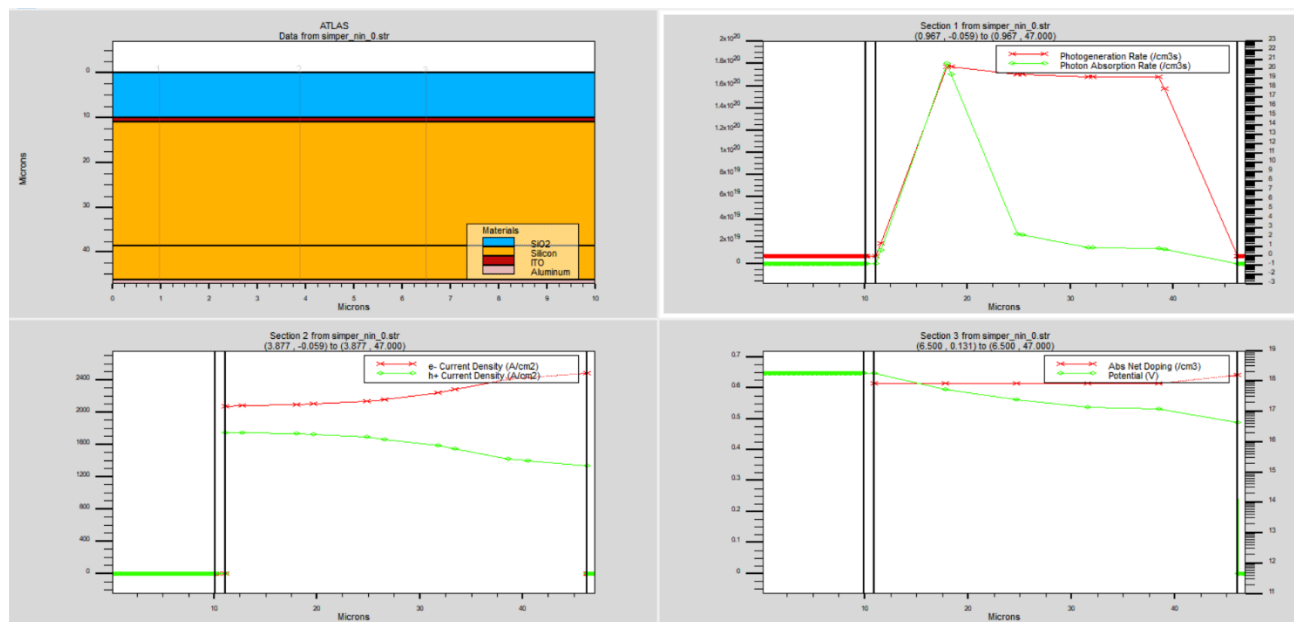


**Figure 22.** Cross-section of the single-homojunction stack (**top left**) with several plots showing photon absorption & photogeneration (**top right**), electron & hole current density (**bottom left**), and absolute net doping & potential (**bottom right**) - in relation to the depth of the stack. In all of these plots, the scale for the line in red is on the right; and the scale for the line in green is on the left. a plot showing depth vs photogeneration & photon absorption rate.

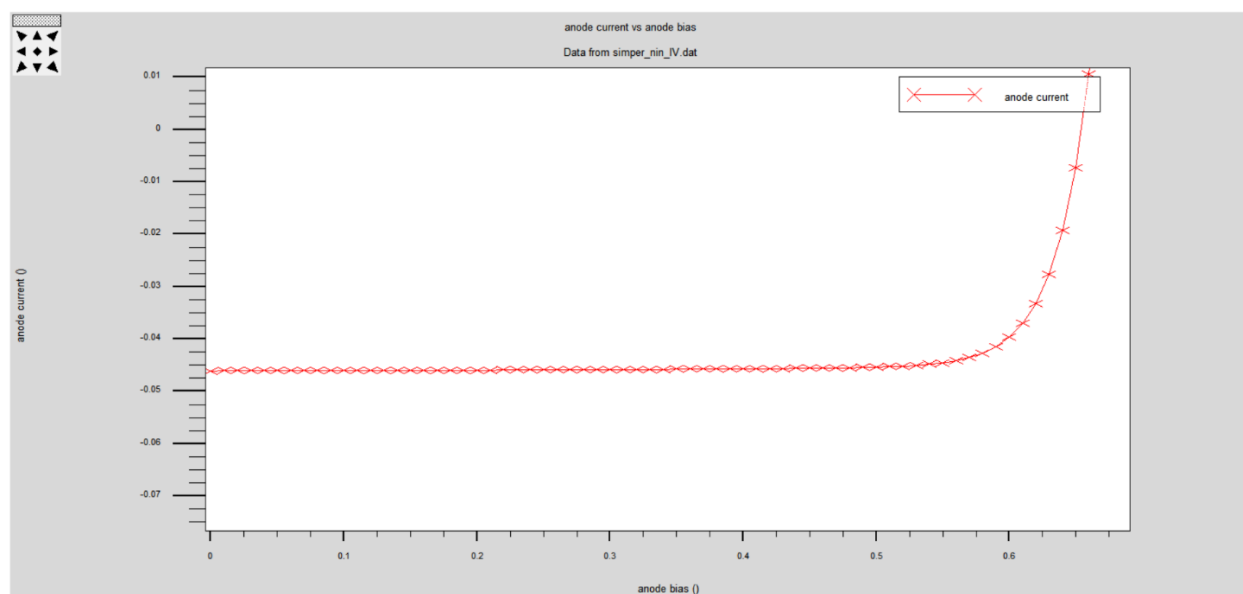


**Figure 23.** I-V data-plot of the single-heterojunction cell

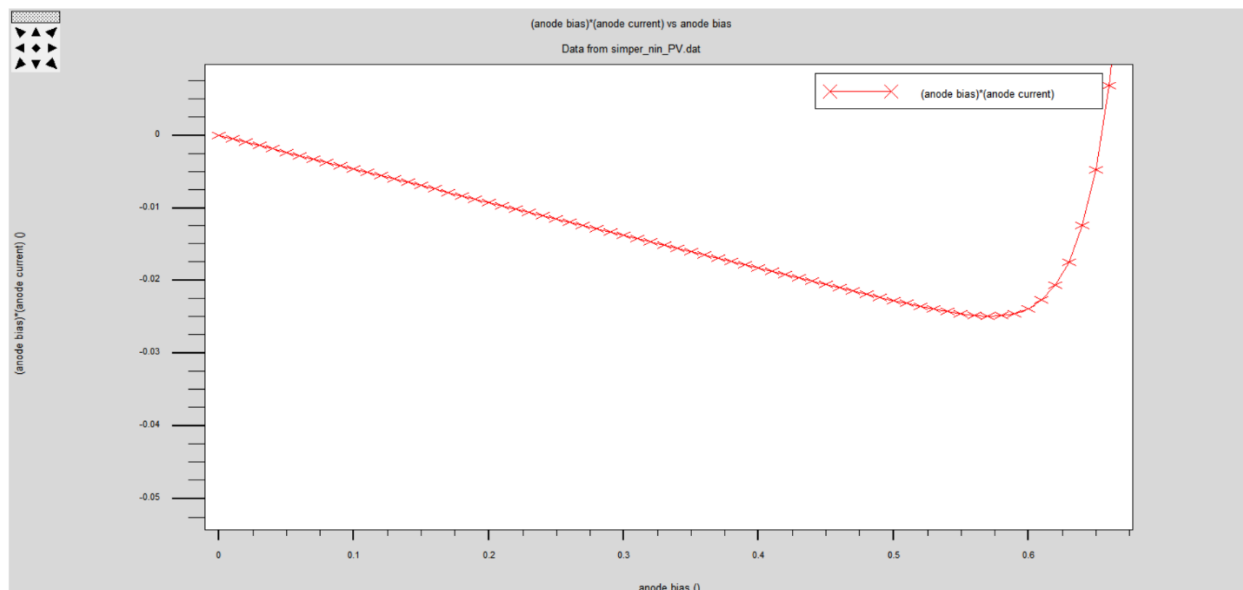


**Figure 24.** P-V data-plot of the single-heterojunction cell

Variables history		
Voc	0.654093732335918	(# 105)
Isc	0.04615811785	(# 106)
Jsc (mA/cm2)	11.539525	(# 107)
Power	9.88131291682493e-324	(# 108)
Pmax	0.0248704780035	(# 109)
V_Pmax	0.57	(# 110)
Fill Factor	0.823751896368969	(# 111)
intens	0.06327479724	(# 112)
Eff	0.0982638427936556	(# 113)

**Figure 25.** Extracted values from the data plots for the single-heterojunction cell

And here are the results for the single-heterojunction cell:

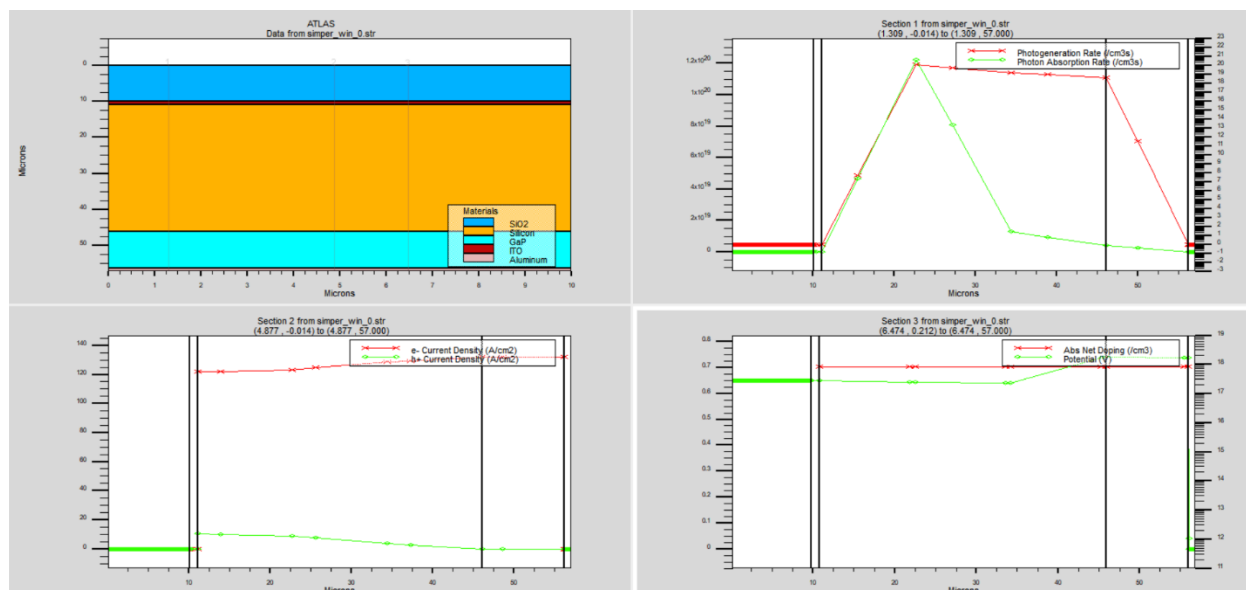


**Figure 26.** Cross-section of the single-heterojunction stack (**top left**) with several plots showing photon absorption & photogeneration (**top right**), electron & hole current density (**bottom left**), and absolute net doping & potential (**bottom right**) - in relation to the depth of the stack. In all of these plots, the scale for the line in red is on the right; and the scale for the line in green is on the left. a plot showing depth vs photogeneration & photon absorption rate.

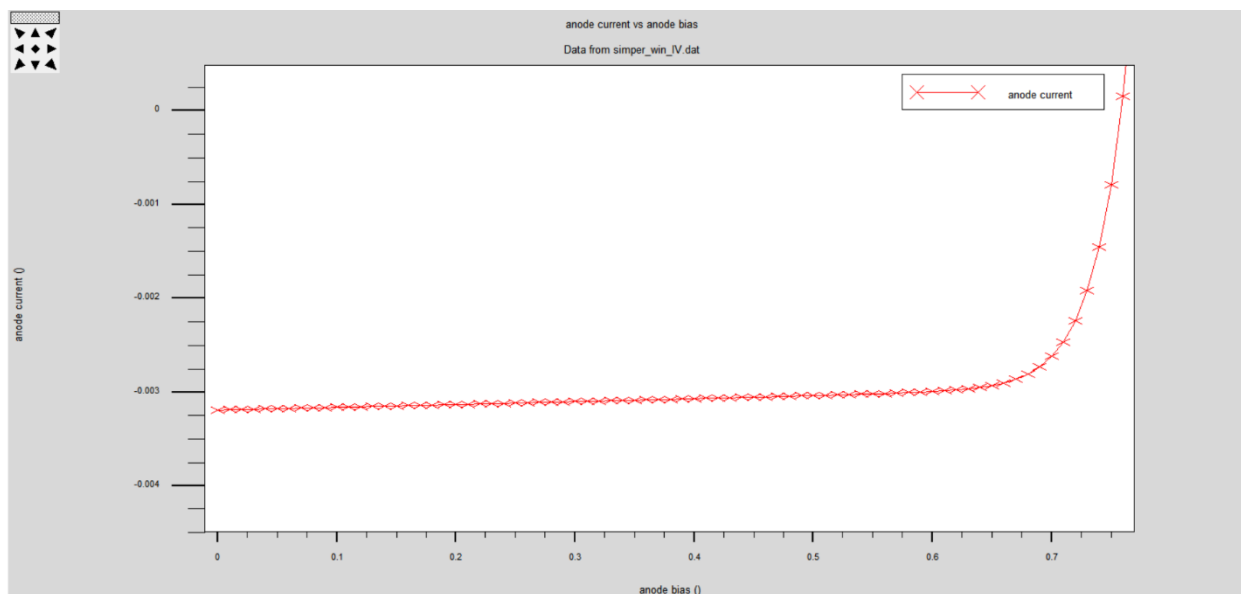


**Figure 27.** I-V data-plot of the single-heterojunction cell



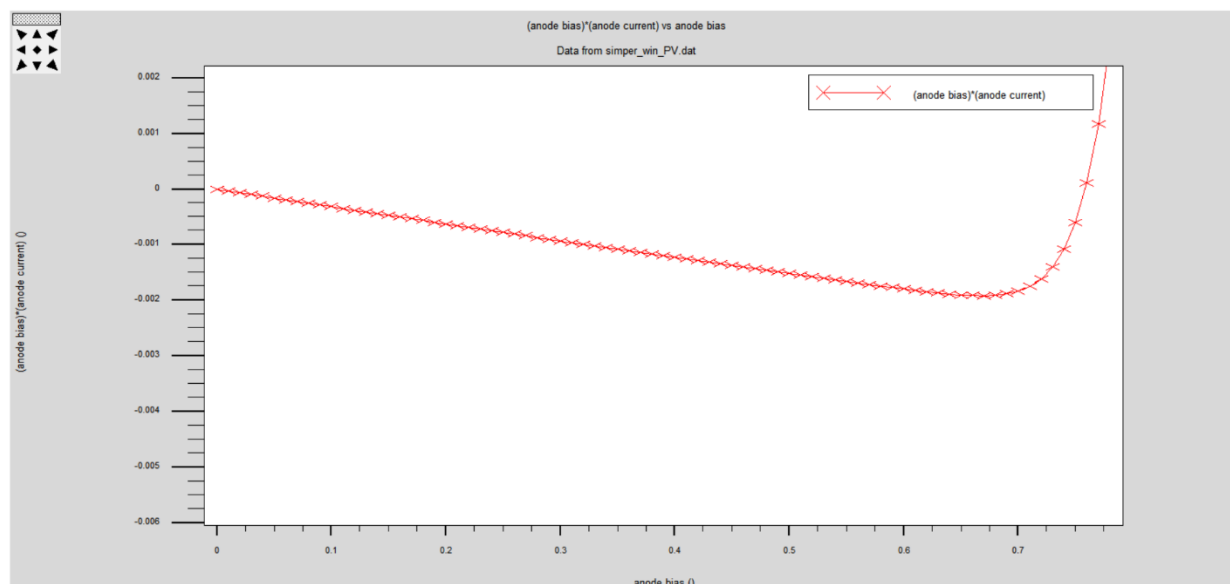


**Figure 28.** P-V data-plot of the single-heterojunction cell

Variables history		
Voc	0.758385691536625	(# 106)
Isc	0.003192996837	(# 107)
Jsc (mA/cm2)	0.79825	(# 108)
Power	9.88131291682493e-324	(# 109)
Pmax	0.00191897769672	(# 110)
V_Pmax	0.67	(# 111)
Fill Factor	0.792467066366994	(# 112)
intens	0.06327479724	(# 113)
Eff	0.007581928350623	(# 114)

**Figure 29.** Extracted values from the data plots for the single-heterojunction cell

By comparing the Voc of **Figure 25** with **Figure 29**, I can validate that voltage can be increased by adding a window, although by this simulation alone I cannot validate to the extent of showing the open-circuit voltage exceeding the built-in voltage. However, this benefit to the voltage comes at a great cost to the current. You can go back and see that the short-circuit current, and hence the maximum power, is nearly ten times greater. I believe the cause of this great loss is due to reflection of photons off of the surfaces in the heterojunction cell, leading to half as many photon absorptions as the homojunction cell (**Figures 22&26, top right**). Also, it seems reasonable to assume that the decrease in electron/hole current density from the homojunction to the heterojunction (**Figures 22&26, bottom left**) is partly due to: the aforementioned loss of light absorption, the loss of an n-region absorber to contribute to current generation, and the lengthening of the p-region which lessens the difference in carrier density over the difference in depth. When the difference in carrier density with depth is lessened in degree, there is less of a ‘pressure

differential' which would act on charge carriers to move via diffusion. Given that the current density in the heterojunction is less than the homojunction by a factor of 16, there are likely still other factors behind this drop in performance that haven't been comprehended. To sum up, maybe the addition of absorber-window heterojunctions is advantageous for *some* designs such as those mentioned in Fonash's text, but that does not seem to be affirmed here. There is now little justification for my research to compare a triple-junction design involving heterojunctions against an analogous triple-homojunction design, given these inconclusive results.

## Parallel vs Series (vs Hybrid)

Perhaps the addition of windows provides no general advantage, but a parallel geometry over a series geometry may still prove superior. The next comparison will be a triple-homojunction solar cell which uses no window materials, in a parallel geometry – against a similar design in a series geometry. The results for the parallel arrangement are as follows:

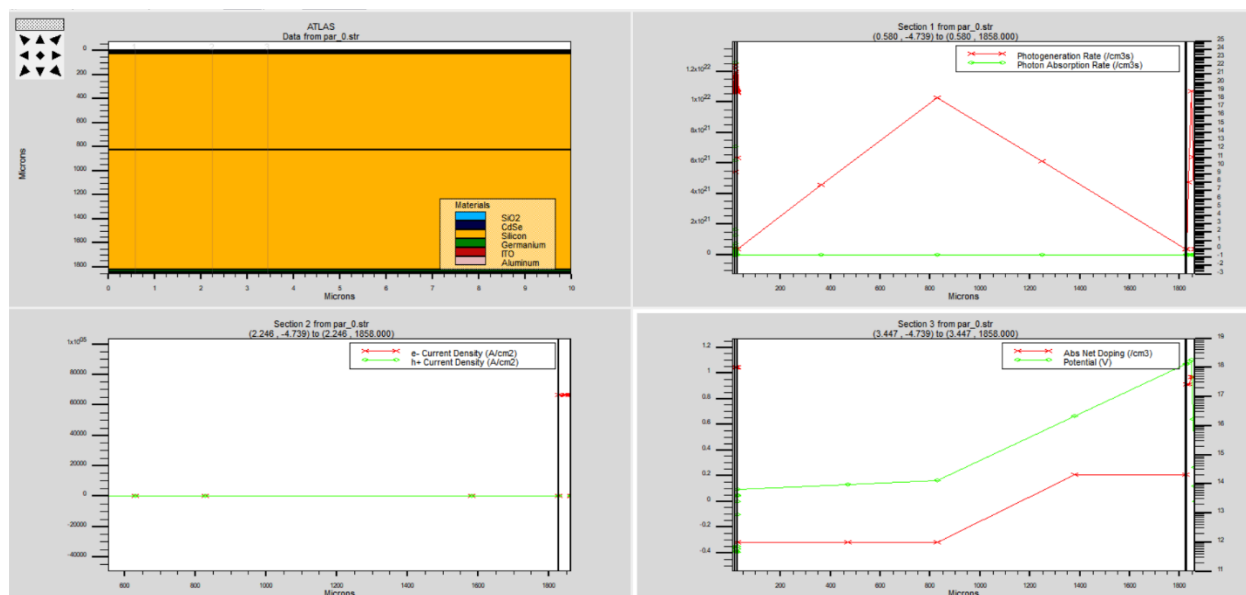


**Figure 30.** Cross-section of the parallel, triple-homojunction stack (**top left**) with several plots showing photon absorption & photogeneration (**top right**), electron & hole current density (**bottom left**), and absolute net doping & potential (**bottom right**) - in relation to the depth of the stack. In all of these plots, the scale for the line in red is on the right; and the scale for the line in green is on the left. a plot showing depth vs photogeneration & photon absorption rate.

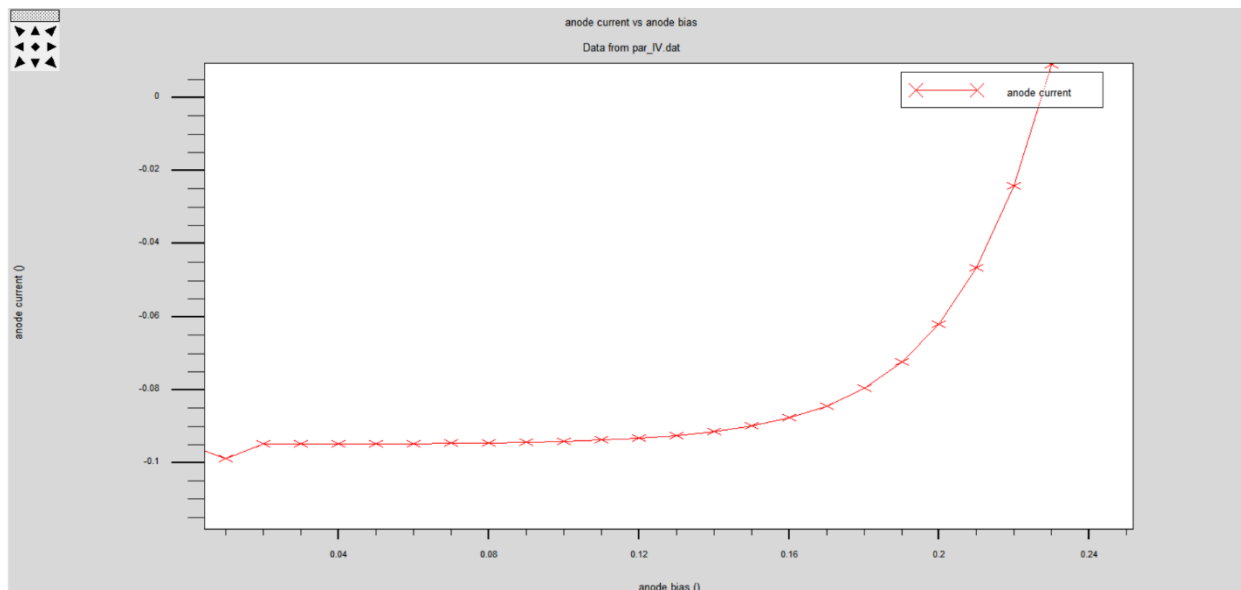


**Figure 31.** I-V data-plot of the parallel, triple-homojunction cell

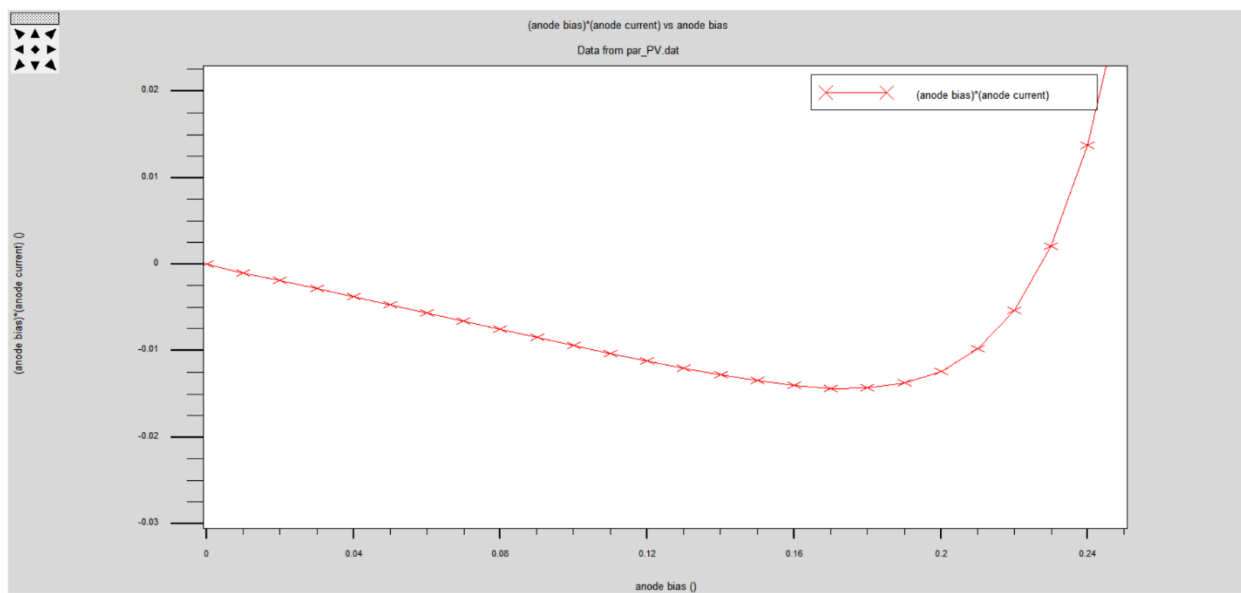


**Figure 32.** P-V data-plot of the parallel, triple-homojunction cell

Variables history		
Voc	0.227324692314693	(# 119)
Isc	0.09489996063	(# 120)
Jsc (mA/cm <sup>2</sup> )	23.725	(# 121)
Power	9.88131291682493e-324	(# 122)
Pmax	0.0143415419261	(# 123)
V_Pmax	0.169998670404634	(# 124)
Fill Factor	0.664784928760379	(# 125)
intens	0.1316056224	(# 126)
Eff	0.0272432487880492	(# 127)

**Figure 33.** Extracted values from the data plots for the parallel, triple-homojunction cell

And the results for the series geometry are:

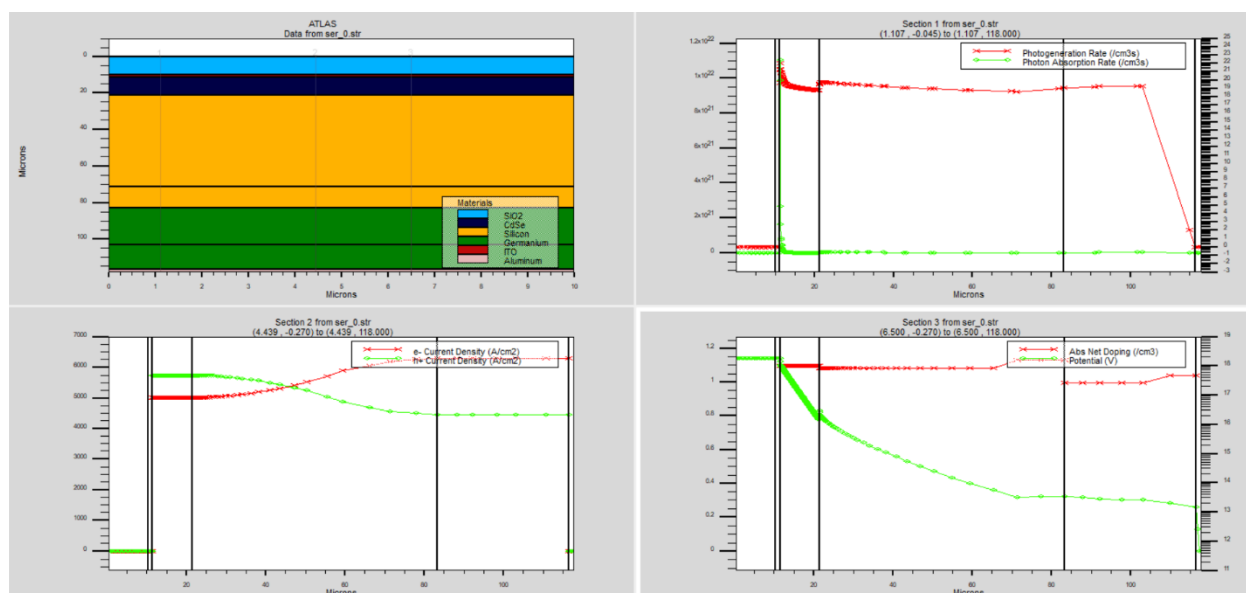


**Figure 34.** Cross-section of the series, triple-homojunction stack (**top left**) with several plots showing photon absorption & photogeneration (**top right**), electron & hole current density (**bottom left**), and absolute net doping & potential (**bottom right**) - in relation to the depth of the stack. In all of these plots, the scale for the line in red is on the right; and the scale for the line in green is on the left. a plot showing depth vs photogeneration & photon absorption rate.

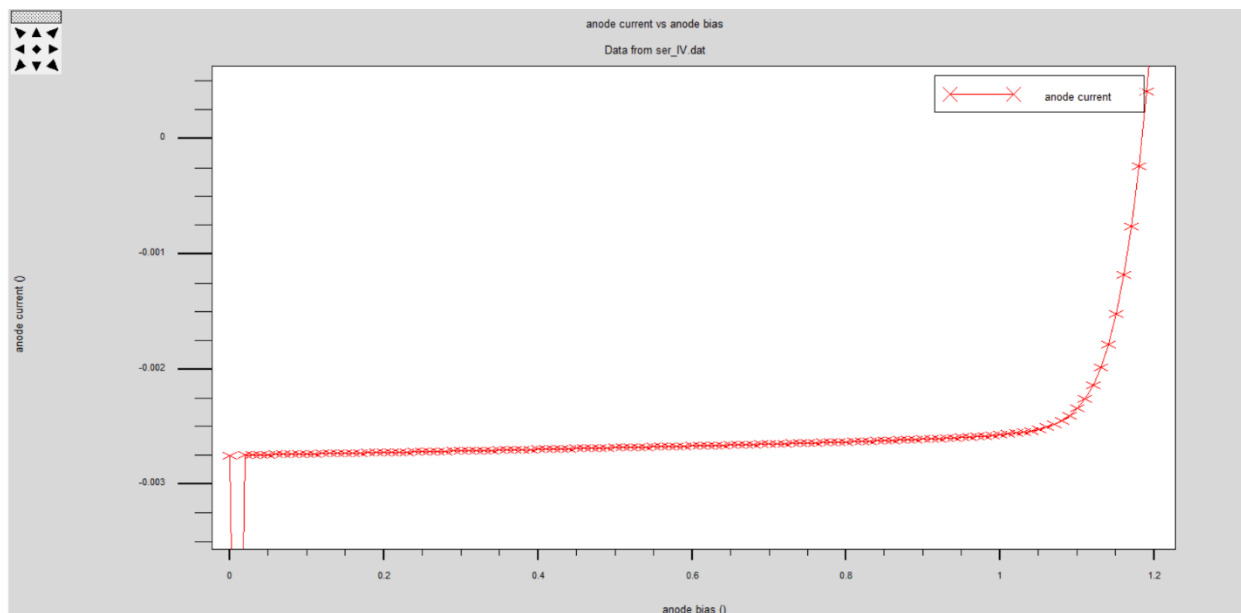


**Figure 35.** I-V data-plot of the series, triple-homojunction cell

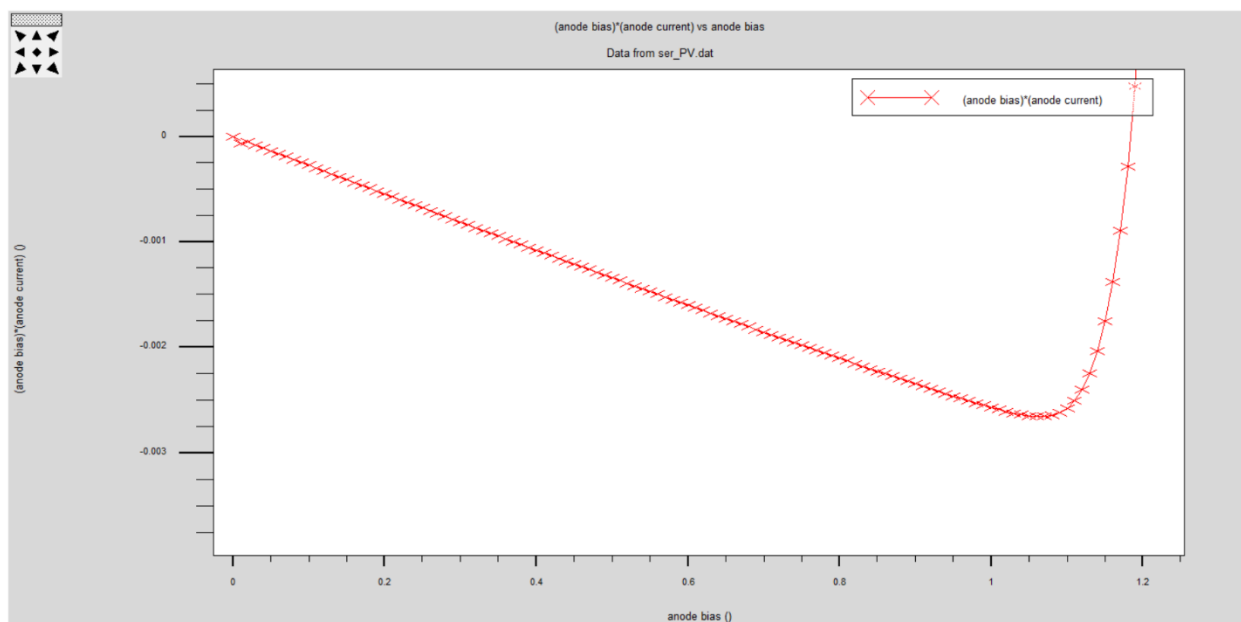


**Figure 36.** P-V data-plot of the series, triple-homojunction cell

Variables history		
Voc	1.18374065481781	(# 114)
Isc	0.002750696715	(# 115)
Jsc (mA/cm2)	0.687675	(# 116)
Power	9.88131291682493e-324	(# 117)
Pmax	0.0026574685904	(# 118)
V_Pmax	1.06	(# 119)
Fill Factor	0.816147810478522	(# 120)
intens	0.1316056224	(# 121)
Eff	0.00504815509931158	(# 122)

**Figure 37.** Extracted values from the data plots for the series, triple-homojunction cell

As expected, the parallel geometry was behind the series cell in terms of open-circuit voltage, but it bested the series cell in short-circuit current so much that it generated a maximum power of nearly six times greater than that of its rival. Also, the reader may have noticed that neither of the two designs are very efficient in comparison with the previously simulated Silicon homojunction. This is principally caused by surface reflection. It is thin, but you may notice from the top right of **Figures 30&34** that photon absorption rate is high near [top] CdSe junction surface, then drastically falls down. Pithy as this cell's output may be, this shouldn't be taken to discourage the idea of multi-junction cells as there is plenty of research that proves multi-junction cells aren't vacuous. Measures to prevent such immense reflection are out there, just not mastered here. What is significant, however, is the besting of the parallel arrangement over the series arrangement. I believe this adds weight to the suggestion that parallel geometries may be more energy efficient in general and ought to be pursued further.

Near the end of my research, an idea occurred to me about making a hybrid structure that connected the Silicon and Germanium homojunctions in series, and then connecting that tandem cell in parallel with the CdSe homojunction. From top to bottom: anode - CdSe-p – CdSe-n – cathode – Si-n – Si-p – Ge-n – Ge-p – anode (then tie the two anodes together). Like so:

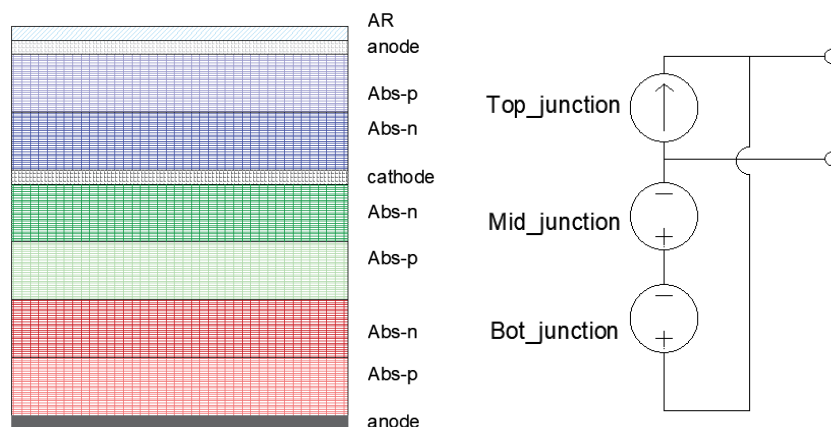


**Figure 38.** Simplified depiction of a solar cell with a hybrid geometry. **Left** is the stack. **Right** is the schematic drawing showing the anodes tied.

Such a design would balance the voltages of the combined output of Ge and Si with the output of CdSe; the disparity in bandgaps is compensated without any windows. Also, the currents would be summed together from the tandem cell and the CdSe junction, and by using one less conducting layer at that. This would seem like the best of both worlds. Such an architecture was put together by re-using the previous calculations for the series and parallel cells. The simulation results turned out to be:

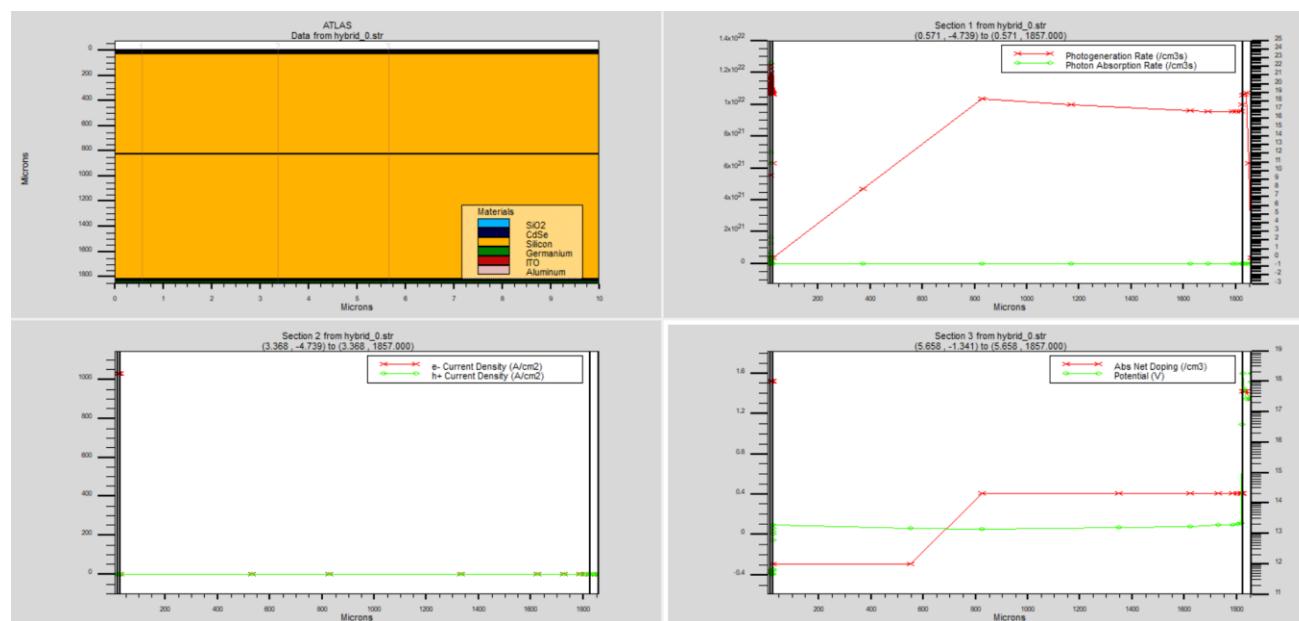


**Figure 39.** Cross-section of the hybrid stack (**top left**) with several plots showing photon absorption & photogeneration (**top right**), electron & hole current density (**bottom left**), and absolute net doping & potential (**bottom right**) - in relation to the depth of the stack. In all of these plots, the scale for the line in red is on the right; and the scale for the line in green is on the left. a plot showing depth vs photogeneration & photon absorption rate.

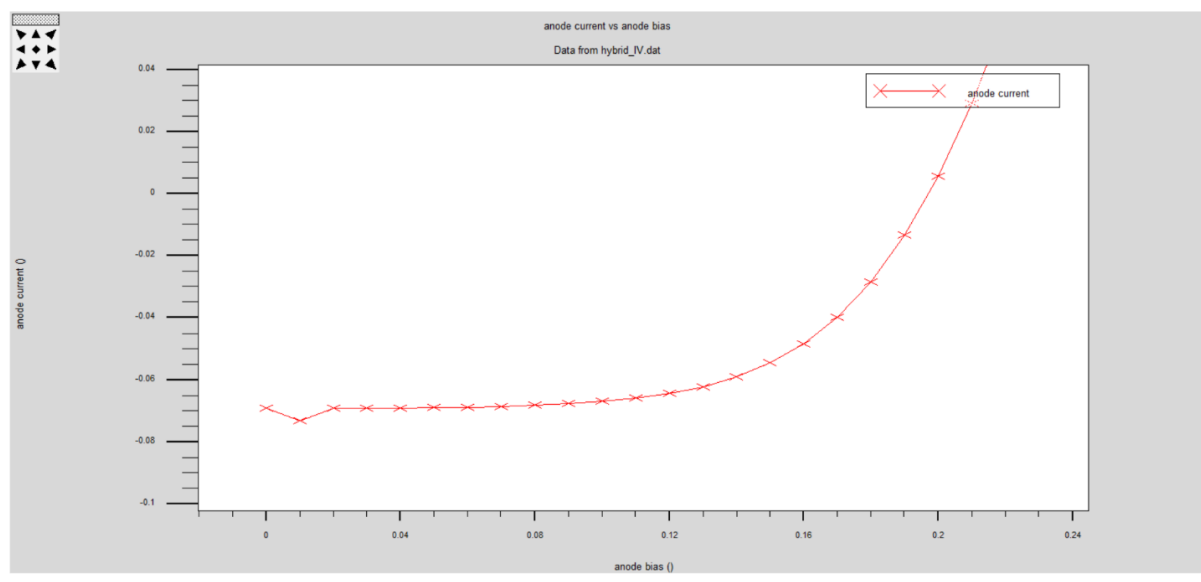


Figure 40. I-V data-plot of the hybrid cell

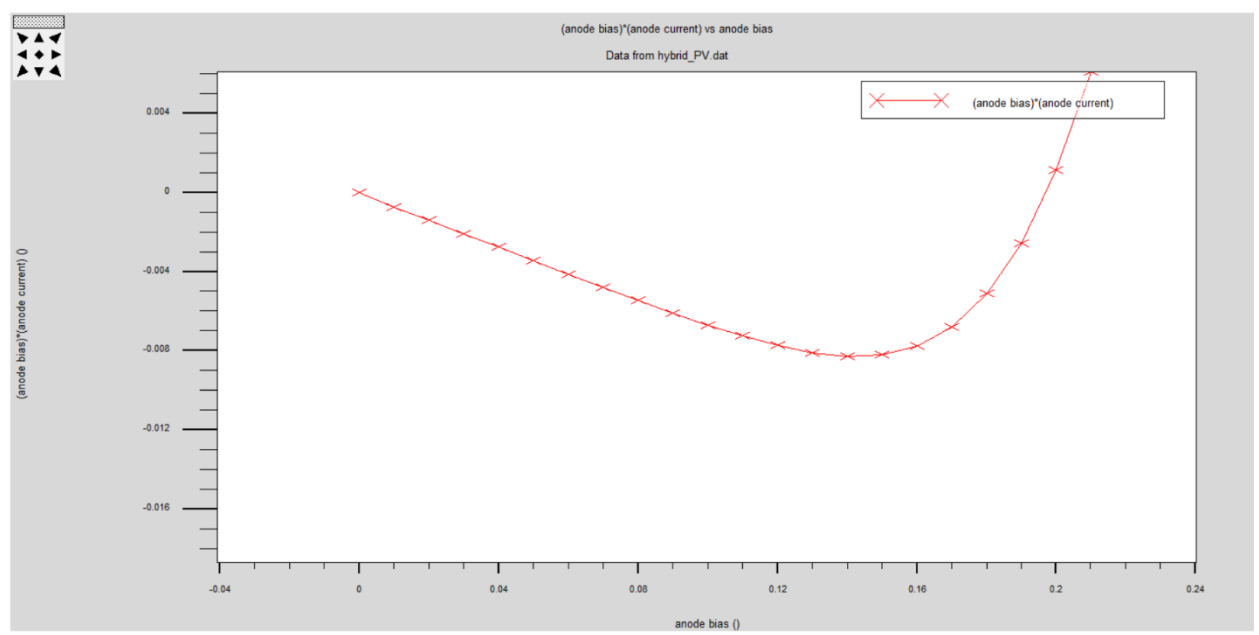
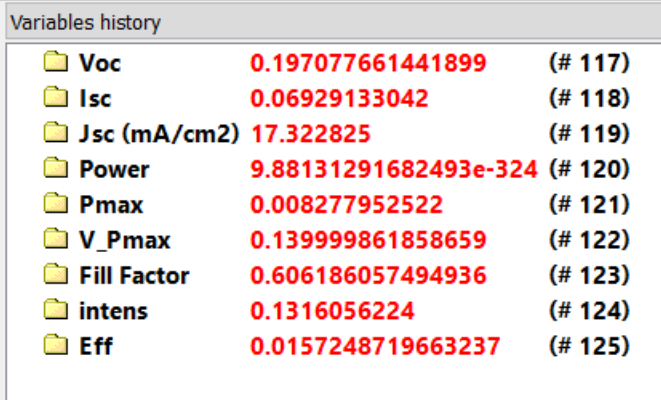


Figure 41. P-V data-plot of the hybrid cell





Variable	Value	Index
Voc	0.197077661441899	(# 117)
Isc	0.06929133042	(# 118)
Jsc (mA/cm2)	17.322825	(# 119)
Power	9.88131291682493e-324	(# 120)
Pmax	0.008277952522	(# 121)
V_Pmax	0.139999861858659	(# 122)
Fill Factor	0.606186057494936	(# 123)
intens	0.1316056224	(# 124)
Eff	0.0157248719663237	(# 125)

**Figure 42.** Extracted values from the data plots for the hybrid cell

Again, emphasizing the last figure, **Figure 41**, the results depict the hybrid cell not being able to match the performance of the purely parallel cell. This was unexpected, though it is still better than the series configuration. Hence, the output at least further advocates including parallel connections in multi-junction solar cells.

## Conclusions

We have just finished an investigation into alternative solar cell structures comparing series vs parallel geometries and windowless vs windowed junctions. I theorized that a structure using windows would increase output voltage and overall output power. As it happens, while the output voltage did increase, it was at the dire expense of the output power and therefore senseless. Parallel geometries, on the other hand, proved superior to the common series design when ran in simulations.

Following this investigation, I desire that others pursue research into windowed cell structures. I would especially advise that hybrid structures, which blend series and parallel connections within the same stack, be further investigated given its soundness in theory. In any case, the bottom line is I insist parallel geometries be developed. I think there is good reason to say parallel geometries outstrip its rivals in terms of output power and hence efficiency.

## Works Cited

- Aggarwal, Vikram. "What are the most efficient solar panels on the market? Solar panel efficiency explained" *energysage*, January 1 2019.
- Dittrich, Thomas. *Material Concepts for Solar Cells. Energy Futures*, vol. 1, Imperial College Press, 2015.
- Fonash, Stephen. *Solar Cell Device Physics*. 2<sup>nd</sup> ed., Academic Press, 2011.
- Ioffe Institute. "New Semiconductor Materials. Characteristics and Properties." *Ioffe Physico-Technical Institute*, 1998
- Jeon, Jin-Woo; Ji, Suk-Yong; Kim, Hoon-Young; Choi, Wonsuk; Shin, Young-Gwan; Cho, Sung-Hak. "Formation of Permanent Brown-colored Patterns in Transparent BK7 Glass upon Irradiation with a Tightly Focused Femtosecond Laser" *Research & Reviews: Journal of Material Sciences*, Department of Laser and Electron Beam Application, Korea Institute of Machinery and Materials. March 29 2018.
- Kurnaiwan, Oka. "Study of a single coaxial silicon nanowire for on-chip integrated photovoltaic application" *ResearchGate*, January 2009.
- Matasci, Sara. "Should I go solar now or wait?" *energysage*, January 1 2019.
- McNamara, Shamus. *Operating Principles of Semiconductor Devices*. University of Louisville, 2016
- Polyanskiy, Mikhail. *RefractiveIndex.INFO*, 2008-2019
- Royal Society of Chemistry. "manuscript" *Royal Society of Chemistry*, 2014. <http://www.rsc.org/suppdata/cp/c3/c3cp54589j/c3cp54589j.pdf>
- Scanlon, David. Walsh, Aron. Watson, Graeme. "Understanding the p-Type Conduction Properties of the Transparent Conducting Oxide CuBO<sub>2</sub>: A Density Functional Theory Analysis" no. 21, *Chemistry of Materials*, 2009.
- Schweber, Bill. "Solar cells and power, Part 2 – power extraction" *Power Electronic Tips*, December 28 2017
- Springer. *II-VI and I-VII Compounds; Semimagnetic Compounds. Semiconductors*, svol. B, *Group III Condensed Matter*, vol. 41, *Landolt-Börnstein: Numerical Data and Functional Relationships in Science and Technology*, Springer, 1999
- Stadler, Andreas. "Transparent Conducting Oxides – An Up-To-Date Overview", no. 5, *Materials*, April 19 2012.

## Appendix

The TCAD software code for the simple, silicon, single-homojunction solar cell:

```
#####
##### Here goes Levi's simple silicon serial solar cell experiment #####
#####
go atlas

# Generate a structured mesh automatically, based on the region statements
mesh auto width=4e7
x.m loc=0.0 s=0.5
x.m loc=10 s=0.5
y.m loc=0 s=0.1
y.m loc=47 s=0.1
# Area = 4 square centimeters

# Declare the non-conductor regions
region num=1 y.min=0 y.max=10.003 material = Oxide
region num=2 y.min=11.003 y.max=38.587 material = Silicon
region num=3 y.min=38.587 y.max=46.189 material = Silicon

# Declare the electrodes
electrode name=anode num=1 y.min=10.003 y.max=11.003 mat=ITO
electrode name=cathode num=2 y.min=46.189 y.max=47.000 mat=Aluminum

# Specify doping
doping region=2 uniform p.type conc=8.519e17
doping region=3 uniform n.type conc=1.599e18

# Declare how the electrodes are arranged into contacts. Here, it's pretty straightforward.
contact name=anode workfunction=5.09 resist=0
contact name=cathode workfunction=4.13 resist=0

# Specify some material properties
material material =Oxide real.index =1.9191 imag.index=0
material material =ITO real.index =2 imag.index=0
material material =Silicon real.index =3.6828 affinity=4.05 eg300=1.12 nc300=3.51e19 nv300=1.87e19

# Model our simulations while taking particular factors into account
# fermi - specifies Fermi-Dirac carrier statistics be used
# conmob - specifies that a concentration dependent mobility be used (for Silicon)
# fldmob - specifies a lateral electric field-dependent model be used
# consrh - Shockley-Reid-Hall recomb with concentration dependent lifetimes
# auger - specifies Auger recombination
# print - prints the status of all models
models fermi conmob fldmob auger print

# Specify the beam. The beam originates 5 microns across and 5 microns up, power is sourced from an example file,
# the dialog window will be descriptive, and light will reflect off of the back contact of the cell. Further, a range of wavelengths is used which
# cannot be absorbed by the window, thus is plays no role in absorption – as intended.
beam num=1 x.o=5 y.o=-5 angle=90 power.file=solarex01.spec wavel.start=.550 wavel.end=1.130 wavel.num=580 verbose back.reflect

# Limit the iterations to 100 and the maximum amount of attempts to trap the output to 25
method itlimit=100 maxtraps=25

# Saves optical intensity to solution files
output opt.int
# Saves the optical intensity for beam number 1 to the log files
probe name=inten beam=1 intensity
```

```

# Compute the results for darkness, setting initial voltages to 0
solve init
# Solve using the previous solution for initial approximations
solve previous

# Here we ramp the beam. This is not to simulate
# sunrise but to insure convergence. Often setting
# an optical source directly to its final value
# can present difficulties in convergence for
# Newton's method so it may be advisable to
# ramp the optical source from a much smaller value.
solve b1=1e-09
solve b1=1e-07
solve b1=1e-05
solve b1=1e-03
solve b1=1e-01
solve b1=1

# Log the following computations
log outfile = simper_nin_0.log

# Solve, setting current to 0 so that open-circuit
# conditions are met.
solve   ianode=0  b1=1   name=anode
# Solve, setting voltage to 0 so that short-circuit
# conditions are met
solve   vanode=0.0  b1=1   name=anode
# Ramp the bias so that I-V characteristics can be extracted
solve   name=anode  b1=1  vstep=0.01  vfinal=1.12

# Save the structure of the cell
save outf=simper_nin_0.str
# Plot structure of the cell
tonyplot simper_nin_0.str

# End logging data
log off

# Extract important figures of merit
extract init infile = "simper_nin_0.log"
extract name="Voc"  abs(x.val from curve(v."anode", i."anode") where y.val=0) outf="simper_nin_IV.dat"
extract name="Isc"  y.val from curve(v."anode", abs(i."anode")) where x.val=0
extract name="Jsc (mA/cm2)"  $"Isc"*1e03/4
extract name="Power"  curve(v."anode", (v."anode" * i."anode" )) outf="simper_nin_PV.dat"
extract name="Pmax"  (-1)*min(curve(v."anode", (v."anode" * i."anode" )))
extract name="V_Pmax"  x.val from curve(v."anode", (v."anode"*i."anode")) where y.val=(-1)*$"Pmax"
extract name="Fill Factor"  ($"Pmax"/($"Isc"*$"Voc"))
extract name="intens"  max(probe."inten")
extract name="Eff"  ($"Pmax"/($"intens"*4))

# Plot IV and PV curves
tonyplot simper_nin_IV.dat
tonyplot simper_nin_PV.dat

quit

```

## The TCAD software code for the simple, silicon, single-heterojunction solar cell:

```
#####
##### Here goes Levi's simple silicon serial solar cell experiment, with windows! #####
#####
go atlas

# Generate a structured mesh automatically, based on the region statements
mesh auto width=4e7
x.m loc=0.0 s=0.5
x.m loc=10 s=0.5
y.m loc=0 s=0.1
y.m loc=57 s=0.1
# Area = 4 square centimeters

# Declare the non-conductor regions
region num=1 y.min=0 y.max=10.003 material = Oxide
region num=2 y.min=11.003 y.max=46.081 material = Silicon
region num=3 y.min=46.081 y.max=56.190 material = GaP

# Declare the electrodes
electrode name=anode num=1 y.min=10.003 y.max=11.003 mat=ITO
electrode name=cathode num=2 y.min=56.190 y.max=57.000 mat=Aluminum

# Specify doping
doping region=2 uniform p.type conc=8.519e17
doping region=3 uniform n.type conc=8.2e17

# Declare how the electrodes are arranged into contacts. Here, it's pretty straightforward.
contact name=anode workfunction=5.09 resist=0
contact name=cathode workfunction=3.88 resist=0

# Specify some material properties
material material =Oxide real.index =1.9191 imag.index=0
material material =ITO real.index =2 imag.index=0
material material =Silicon real.index =3.6828 affinity=4.05 eg300=1.12 nc300=3.51e19 nv300=1.87e19
material material =GaP real.index =3.2046 affinity=3.8 eg300=2.26 nc300=1.8e19 nv300=1.9e19

# Model our simulations while taking particular factors into account
# fermi - specifies Fermi-Dirac carrier statistics be used
# conmob - specifies that a concentration dependent mobility be used (for Silicon)
# fldmob - specifies a lateral electric field-dependent model be used
# consrh - Shockley-Reid-Hall recomb with concentration dependent lifetimes
# auger - specifies Auger recombination
# print - prints the status of all models
models fermi conmob fldmob auger print

# Specify the beam. The beam originates 5 microns across and 5 microns up, power is sourced from an example file,
# the dialog window will be descriptive, and light will reflect off of the back contact of the cell. Further, a range of wavelengths is used which
# cannot be absorbed by the window, thus it plays no role in absorption – as intended.
beam num=1 x.o=5 y.o=-5 angle=90 power.file=solarex01.spec wavel.start=.550 wavel.end=1.130 wavel.num=580 verbose back.reflect

# Limit the iterations to 100 and the maximum amount of attempts to trap the output to 25
method itlimit=100 maxtraps=25

# Saves optical intensity to solution files
output opt.int
# Saves the optical intensity for beam number 1 to the log files
probe name=inten beam=1 intensity

# Compute the results for darkness, setting initial voltages to 0
solve init
# Solve using the previous solution for initial approximations
```

solve previous

```

# Here we ramp the beam. This is not to simulate
# sunrise but to insure convergence. Often setting
# an optical source directly to its final value
# can present difficulties in convergence for
# Newton's method so it may be advisable to
# ramp the optical source from a much smaller value.
solve b1=1e-09
solve b1=1e-07
solve b1=1e-05
solve b1=1e-03
solve b1=1e-01
solve b1=1

# Log the following computations
log outfile = simper_win_0.log

# Solve, setting current to 0 so that open-circuit
# conditions are met.
solve   ianode=0  b1=1    name=anode
# Solve, setting voltage to 0 so that short-circuit
# conditions are met
solve   vanode=0.0  b1=1    name=anode
# Ramp the bias so that I-V characteristics can be extracted
solve   name=anode  b1=1    vstep=0.01  vfinal=1.12

# Save the structure of the cell
save outf=simper_win_0.str
# Plot structure of the cell
tonyplot simper_win_0.str

# End logging data
log off

# Extract important figures of merit
extract init infile = "simper_win_0.log"
extract name="Voc" abs(x.val from curve(v."anode", i."anode") where y.val=0) outf="simper_win_IV.dat"
extract name="Isc" y.val from curve(v."anode", abs(i."anode")) where x.val=0
extract name="Jsc (mA/cm2)" $("Isc"*1e03/4)
extract name="Power" curve(v."anode", (v."anode" * i."anode" )) outf="simper_win_PV.dat"
extract name="Pmax" (-1)*min(curve(v."anode", (v."anode" * i."anode" )))
extract name="V_Pmax" x.val from curve(v."anode", (v."anode"*i."anode")) where y.val=(-1)*$("Pmax"
extract name="Fill Factor" ($"Pmax"/($"Isc"*$"Voc"))
extract name="intens" max(probe."inten")
extract name="Eff" ($"Pmax"/($"intens"*4))

# Plot IV and PV curves
tonyplot simper_win_IV.dat
tonyplot simper_win_PV.dat

quit

```

## The TCAD software code for the parallel, triple-homojunction solar cell:

```
#####
##### Here goes Levi's parallel solar cell experiment, without windows! #####
#####
go atlas

# Generate a structured mesh automatically, based on the region statements
mesh auto width=4e7
x.m loc=0.0 s=1
x.m loc=10 s=1
y.m loc=0 s=1
y.m loc=1858 s=1
# Area = 4 square centimeters

# Declare the non-conductor regions
region num=1 y.min=0 y.max=10.092 material = Oxide
region num=2 y.min=11.142 y.max=21.089 material = CdSe
region num=3 y.min=21.089 y.max=21.203 material = CdSe
region num=4 y.min=22.253 y.max=822.111 material = Silicon
region num=5 y.min=822.111 y.max=1822.081 material = Silicon
region num=6 y.min=1823.281 y.max=1843.174 material = Germanium
region num=7 y.min=1843.174 y.max=1856.560 material = Germanium

# Declare the electrodes
electrode name=anode num=1 y.min=10.092 y.max=11.142 mat=ITO
electrode name=cathode2 num=2 y.min=21.203 y.max=22.253 mat=ITO
electrode name=anode2 num=3 y.min=1822.081 y.max=1823.281 mat=ITO
electrode name=cathode num=4 y.min=1856.560 y.max=1858.000 mat=Aluminum

# Specify doping
doping region=2 uniform p.type conc=1.0e18
doping region=3 uniform n.type conc=1.0e18
doping region=4 uniform n.type conc=1e12
doping region=5 uniform p.type conc=2e14
doping region=6 uniform p.type conc=2.569e17
doping region=7 uniform n.type conc=4.65e17

# Declare how the electrodes are arranged into contacts. Here, it's pretty straightforward.
contact name=anode workfunction=6.30 resist=0
contact name=cathode2 common=cathode short workfunction=4.25 resist=0
contact name=anode2 common=anode short workfunction=4.87 resist=0
contact name=cathode workfunction=4.08 resist=0

# Specify some material properties
material material =Oxide real.index =1.9191 imag.index=0
material material =ITO real.index =2 imag.index=0
material material =CdSe real.index =2.624 affinity=4.7 eg300=1.68
material material =Silicon real.index =3.6828 affinity=4.05 eg300=1.12 nc300=3.51e19 nv300=1.87e19
material material =GaP real.index =3.2046 affinity=3.8 eg300=2.26 nc300=1.8e19 nv300=1.9e19

# Model our simulations while taking particular factors into account
# fermi - specifies Fermi-Dirac carrier statistics be used
# conmob - specifies that a concentration dependent mobility be used (for Silicon)
# fldmob - specifies a lateral electric field-dependent model be used
# consrh - Shockley-Reid-Hall recomb with concentration dependent lifetimes
# auger - specifies Auger recombination
# print - prints the status of all models
models fermi conmob fldmob auger print

# Specify the beam. The beam originates 5 microns across and 5 microns up, power is sourced from an example file,
# the dialog window will be descriptive, and light will reflect off of the back contact of the cell.
beam num=1 x.o=5 y.o=5 angle=90 power.file=solarex01.spec verbose back.reflect
```



```

# Limit the iterations to 100 and the maximum amount of attempts to trap the output to 25
method itlimit=100 maxtraps=25

# Saves optical intensity to solution files
output opt.int
# Saves the optical intensity for beam number 1 to the log files
probe name=inten beam=1 intensity

# Compute the results for darkness, setting initial voltages to 0
solve init
# Solve using the previous solution for initial approximations
solve previous

# Here we ramp the beam. This is not to simulate
# sunrise but to insure convergence. Often setting
# an optical source directly to its final value
# can present difficulties in convergence for
# Newton's method so it may be advisable to
# ramp the optical source from a much smaller value.
solve b1=1e-09
solve b1=1e-07
solve b1=1e-05
solve b1=1e-03
solve b1=1e-01
solve b1=1

# Log the following computations
log outfile = par_0.log

# Solve, setting current to 0 so that open-circuit
# conditions are met.
solve ianode=0 b1=1 name=anode
# Solve, setting voltage to 0 so that short-circuit
# conditions are met
solve vanode=0.0 b1=1 name=anode
# Ramp the bias so that I-V characteristics can be extracted
solve name=anode b1=1 vstep=0.01 vfinal=1.60

# Save the structure of the cell
save outf=par_0.str
# Plot structure of the cell
tonyplot par_0.str

# End logging data
log off

# Extract important figures of merit
extract init infile = "par_0.log"
extract name="Voc" abs(x.val from curve(v."anode", i."anode") where y.val=0) outf="par_IV.dat"
extract name="Isc" y.val from curve(v."anode", abs(i."anode")) where x.val=0
extract name="Jsc (mA/cm2)"  $\frac{I_{sc}}{4}$ 
extract name="Power" curve(v."anode", (v."anode" * i."anode" )) outf="par_PV.dat"
extract name="Pmax" (-1)*min(curve(v."anode", (v."anode" * i."anode" )))
extract name="V_Pmax" x.val from curve(v."anode", (v."anode"*i."anode")) where y.val=(-1)*Pmax
extract name="Fill Factor" ( $\frac{P_{max}}{I_{sc} * V_{oc}}$ )
extract name="intens" max(probe."inten")
extract name="Eff" ( $\frac{P_{max}}{intens * 4}$ )

# Plot IV and PV curves
tonyplot par_IV.dat
tonyplot par_PV.dat

quit

```

## The TCAD software code for the series, triple-homojunction solar cell:

```
#####
##### Here goes Levi's series solar cell experiment, without windows! #####
#####
go atlas

# Generate a structured mesh automatically, based on the region statements
mesh auto width=4e7
x.m loc=0.0 s=1
x.m loc=10 s=1
y.m loc=0 s=1
y.m loc=118 s=1
# Area = 4 square centimeters

# Declare the non-conductor regions
region num=1 y.min=0 y.max=10.092 material = Oxide
region num=2 y.min=11.142 y.max=21.089 material = CdSe
region num=3 y.min=21.089 y.max=21.203 material = CdSe
region num=4 y.min=21.203 y.max=71.084 material = Silicon
region num=5 y.min=71.084 y.max=83.002 material = Silicon
region num=6 y.min=83.002 y.max=102.895 material = Germanium
region num=7 y.min=102.895 y.max=116.281 material = Germanium

# Declare the electrodes
electrode name=anode num=1 y.min=10.092 y.max=11.142 mat=ITO
electrode name=cathode num=4 y.min=116.281 y.max=118.000 mat=Aluminum

# Specify doping
doping region=2 uniform p.type conc=1.0e18
doping region=3 uniform n.type conc=1.0e18
doping region=4 uniform p.type conc=8.519e17
doping region=5 uniform n.type conc=1.599e18
doping region=6 uniform p.type conc=2.569e17
doping region=7 uniform n.type conc=4.647e17

# Declare how the electrodes are arranged into contacts. Here, it's pretty straightforward.
contact name=anode workfunction=6.30 resist=0
contact name=cathode workfunction=4.08 resist=0

# Specify some material properties
material material =Oxide real.index =1.9191 imag.index=0
material material =ITO real.index =2 imag.index=0
material material =CdSe real.index =2.624 affinity=4.7 eg300=1.68
material material =Silicon real.index =3.6828 affinity=4.05 eg300=1.12 nc300=3.51e19 nv300=1.87e19
material material =GaP real.index =3.2046 affinity=3.8 eg300=2.26 nc300=1.8e19 nv300=1.9e19

# Model our simulations while taking particular factors into account
# fermi - specifies Fermi-Dirac carrier statistics be used
# conmob - specifies that a concentration dependent mobility be used (for Silicon)
# fldmob - specifies a lateral electric field-dependent model be used
# consrh - Shockley-Reid-Hall recomb with concentration dependent lifetimes
# auger - specifies Auger recombination
# print - prints the status of all models
models fermi conmob fldmob auger print

# Specify the beam. The beam originates 5 microns across and 5 microns up, power is sourced from an example file,
# the dialog window will be descriptive, and light will reflect off of the back contact of the cell.
beam num=1 x.o=5 y.o=-5 angle=90 power.file=solarex01.spec verbose back.reflect

# Limit the iterations to 100 and the maximum amount of attempts to trap the output to 25
method itlimit=100 maxtraps=25

# Saves optical intensity to solution files
```

```

output opt.int
# Saves the optical intensity for beam number 1 to the log files
probe name=inten    beam=1 intensity

# Compute the results for darkness, setting initial voltages to 0
solve init
# Solve using the previous solution for initial approximations
solve previous

# Here we ramp the beam. This is not to simulate
# sunrise but to insure convergence. Often setting
# an optical source directly to its final value
# can present difficulties in convergence for
# Newton's method so it may be advisable to
# ramp the optical source from a much smaller value.
solve b1=1e-09
solve b1=1e-07
solve b1=1e-05
solve b1=1e-03
solve b1=1e-01
solve b1=1

# Log the following computations
log outfile = ser_0.log

# Solve, setting current to 0 so that open-circuit
# conditions are met.
solve    ianode=0 b1=1    name=anode
# Solve, setting voltage to 0 so that short-circuit
# conditions are met
solve    vanode=0.0 b1=1    name=anode
# Ramp the bias so that I-V characteristics can be extracted
solve    name=anode b1=1 vstep=0.01 vfinal=3.10

# Save the structure of the cell
save outf=ser_0.str
# Plot structure of the cell
tonyplot ser_0.str

# End logging data
log off

# Extract important figures of merit
extract init infile = "ser_0.log"
extract name="Voc" abs(x.val from curve(v."anode", i."anode") where y.val=0) outf="ser_IV.dat"
extract name="Isc" y.val from curve(v."anode", abs(i."anode")) where x.val=0
extract name="Jsc (mA/cm2)" "$Isc"*1e03/4
extract name="Power" curve(v."anode", (v."anode" * i."anode" )) outf="ser_PV.dat"
extract name="Pmax" (-1)*min(curve(v."anode", (v."anode" * i."anode" )))
extract name="V_Pmax" x.val from curve(v."anode", (v."anode"*i."anode")) where y.val=(-1)*$Pmax"
extract name="Fill Factor" ($Pmax"/($Isc"*$Voc"))
extract name="intens" max(probe."inten")
extract name="Eff" ($Pmax"/($intens"*4))

# Plot IV and PV curves
tonyplot ser_IV.dat
tonyplot ser_PV.dat

quit

```

## The TCAD software code for the hybrid solar cell:

```
#####
##### Here goes Levi's hybrid solar cell experiment, emphasizing current! #####
#####
go atlas

# Generate a structured mesh automatically, based on the region statements
mesh auto width=4e7
x.m loc=0.0 s=1
x.m loc=10 s=1
y.m loc=0 s=1
y.m loc=1857 s=1
# Area = 4 square centimeters

# Declare the non-conductor regions
region num=1 y.min=0 y.max=10.092 material = Oxide
region num=2 y.min=11.142 y.max=21.089 material = CdSe
region num=3 y.min=21.089 y.max=21.203 material = CdSe
region num=4 y.min=22.253 y.max=822.111 material = Silicon
region num=5 y.min=822.111 y.max=1822.081 material = Silicon
region num=6 y.min=1822.081 y.max=1835.467 material = Germanium
region num=7 y.min=1835.467 y.max=1855.360 material = Germanium

# Declare the electrodes
electrode name=anode num=1 y.min=10.092 y.max=11.142 mat=ITO
electrode name=cathode num=2 y.min=21.203 y.max=22.253 mat=ITO
electrode name=anode2 num=3 y.min=1855.360 y.max=1857.000 mat=Aluminum

# Specify doping
doping region=2 uniform p.type conc=1.0e18
doping region=3 uniform n.type conc=1.0e18
doping region=4 uniform n.type conc=1e12
doping region=5 uniform p.type conc=2e14
doping region=6 uniform n.type conc=4.65e17
doping region=7 uniform p.type conc=2.569e17

# Declare how the electrodes are arranged into contacts. Here, it's pretty straightforward.
contact name=anode workfunction=6.30 resist=0
contact name=cathode workfunction=4.25 resist=0
contact name=anode2 workfunction=4.59 resist=0 common=anode short

# Specify some material properties
material material =Oxide real.index =1.9191 imag.index=0
material material =ITO real.index =2 imag.index=0
material material =CdSe real.index =2.624 affinity=4.7 eg300=1.68
material material =Silicon real.index =3.6828 affinity=4.05 eg300=1.12 nc300=3.51e19 nv300=1.87e19
material material =GaP real.index =3.2046 affinity=3.8 eg300=2.26 nc300=1.8e19 nv300=1.9e19

# Model our simulations while taking particular factors into account
# fermi - specifies Fermi-Dirac carrier statistics be used
# conmob - specifies that a concentration dependent mobility be used (for Silicon)
# fldmob - specifies a lateral electric field-dependent model be used
# consrh - Shockley-Reid-Hall recomb with concentration dependent lifetimes
# auger - specifies Auger recombination
# print - prints the status of all models
models fermi conmob fldmob auger print

# Specify the beam. The beam originates 5 microns across and 5 microns up, power is sourced from an example file,
# the dialog window will be descriptive, and light will reflect off of the back contact of the cell.
beam num=1 x.o=5 y.o=-5 angle=90 power.file=solarex01.spec verbose back.reflect

# Limit the iterations to 100 and the maximum amount of attempts to trap the output to 25
method itlimit=100 maxtraps=25
```

```

# Saves optical intensity to solution files
output opt.int
# Saves the optical intensity for beam number 1 to the log files
probe name=inten    beam=1 intensity

# Compute the results for darkness, setting initial voltages to 0
solve init
# Solve using the previous solution for initial approximations
solve previous

# Here we ramp the beam. This is not to simulate
# sunrise but to insure convergence. Often setting
# an optical source directly to its final value
# can present difficulties in convergence for
# Newton's method so it may be advisable to
# ramp the optical source from a much smaller value.
solve b1=1e-09
solve b1=1e-07
solve b1=1e-05
solve b1=1e-03
solve b1=1e-01
solve b1=1

# Log the following computations
log outfile = hybrid_0.log

# Solve, setting current to 0 so that open-circuit
# conditions are met.
solve   ianode=0  b1=1    name=anode
# Solve, setting voltage to 0 so that short-circuit
# conditions are met
solve   vanode=0.0  b1=1    name=anode
# Ramp the bias so that I-V characteristics can be extracted
solve   name=anode  b1=1  vstep=0.01  vfinal=1.60

# Save the structure of the cell
save outf=hybrid_0.str
# Plot structure of the cell
tonyplot hybrid_0.str

# End logging data
log off

# Extract important figures of merit
extract init infile = "par_0.log"
extract name="Voc" abs(x.val from curve(v."anode", i."anode") where y.val=0) outf="hybrid_IV.dat"
extract name="Isc" y.val from curve(v."anode", abs(i."anode")) where x.val=0
extract name="Jsc (mA/cm2)" "$Isc"*1e03/4
extract name="Power" curve(v."anode", (v."anode" * i."anode" )) outf="hybrid_PV.dat"
extract name="Pmax" (-1)*min(curve(v."anode", (v."anode" * i."anode" )))
extract name="V_Pmax" x.val from curve(v."anode", (v."anode"*i."anode")) where y.val=(-1)*$Pmax"
extract name="Fill Factor" ($Pmax)/($Isc*$Voc))
extract name="intens" max(probe."inten")
extract name="Eff" ($Pmax)/($intens*4)

# Plot IV and PV curves
tonyplot hybrid_IV.dat
tonyplot hybrid_PV.dat

quit

```